5-2018

Degradation of trihalomethanes and choramines by UV and VUV irradiation

Kehui Zhang
Purdue University

DEGRADATION OF TRIHALOMETHANES AND CHLORAMINES BY UVC AND VUV IRRADIATION

by

Kehui Zhang

A Thesis

Submitted to the Faculty of Purdue University

In Partial Fulfillment of the Requirements for the degree of

Master of Science in Environmental and Ecological Engineering

Lyles School of Civil Engineering

West Lafayette, Indiana

May 2018

THE PURDUE UNIVERSITY GRADUATE SCHOOL
STATEMENT OF COMMITTEE APPROVAL

Dr. Ernest R. Blatchley III

Department of Civil Engineering

Dr. Amisha Shah

Department of Civil Engineering

Dr. Chad Jafvert

Department of Civil Engineering

Approved by:

Dr. John Sutherland

Head of Environmental and Ecological Engineering

ACKNOWLEDGMENTS

I would like to thank my advisor and committee members, Dr. Ernest R. Blatchley III, Dr. Chad T. Jafvert and Dr. Amisha Shah for the excellent mentorship during the graduate life. Also, I would like to thank Dr. Mengkai Li for his help and guidance. In addition, I would like to thank lab managers of Civil Engineering and Chemistry Department, Dr. Zyaykina Nadya and Dr. Patricia Bishop for great counseling about technical questions. I would like to thank my group members, Lester T Lee, Xing Li, Moshan Chen and Margaret M Busse for wonderful cooperation.

TABLE OF CONTENTS

LIST OF TABLES

LIST OF FIGURES

ABSTRACT

Author: Zhang, Kehui MS
Institution: Purdue University
Degree Received: May 2018
Title: Degradation of Trihalomethanes and Chloramines by UVC and VUV Irradiation
Major Professor: Ernest R. Blatchley III.

Disinfection byproducts (DBPs) generated from the chlorination of natural organic matter (NOM) represent a source of concern related to drinking water quality. Vacuum-ultraviolet (VUV λ<200 nm), irradiation can be an efficient advanced oxidation process (AOP), has been documented to inactivate pathogens as well as remove micropollutants in drinking water. To compare the effects of VUV and UVC irradiation, four trihalomethanes (THMs) and three chloramines, chloroform ($CHCl_3$), dichlorobromomethane ($CHBrCl_2$), dibromochloromethane ($CHBr_2Cl$), bromoform ($CHBr_3$), monochloramine (NH_2Cl), dichloramine ($NHCl_2$) and trichloramine (NCl_3), were prepared and analyzed for their degradation reaction rate constant under UVC, VUV/UVC, UVC/Cl_2, VUV/UVC/Cl_2 processes. A mini-fluidic VUV/UVC photoreaction system (MVPS) was connected directly to a membrane introduction mass spectrometry (MIMS) for many of these experiments to quickly quantify volatile DBPs dynamic behavior. VUV-UVC absorption spectra (180-300 nm) were measured four THMs. THMs and chloramines were found to be degraded faster by VUV irradiation than by UV irradiation. $CHBr_3$ and NCl_3 were the fastest degraded compound among THMs and chloramines, respectively. In addition, degradation of total THM as well as trihalomethane formation potential (THMFP) generated from the chlorination of humic acid in the presence of bromide with UVC or VUV irradiation were examined; therefore, specific THM species were also quantified and summarized. Finally, 77% reduction in THMFP was

observed in VUV/UVC/Cl_2 process and 82% reduction in total THMs was observed in VUV/UVC process.

INTRODUCTION

Chlorine, a common beneficial disinfectant, is used to inactivate harmful pathogens in water treatment; however, disinfection is accompanied by formation of by-products (DBPs), often from chlorination of natural organic matter (NOM).

Trihalomethanes (THMs) and chloramines, comprising chloroform ($CHCl_3$), dichlorobromomethane ($CHBrCl_2$), dibromochloromethane ($CHBr_2Cl$), bromoform ($CHBr_3$), monochloramine (NH_2Cl), dichloramine ($NHCl_2$) and trichloramine (NCl_3). are important volatile DBPs in many water treatment settings. Long-term exposure to THMs in drinking water or swimming pool has been associated with adverse effects on human health and people are influenced via dermal absorption, inhalation and ingestion during cooking, drinking and showering (Villanueva et al., 2006). Bladder cancer, along with reproduction problems, have been associated with the acute or chronic exposures to THMs (Kumar et al., 2014; Villanueva et al., 2006). Center of Disease Control and Prevention (CDC) reported that chloramines were more likely found in swimming pool other than in drinking water, resulting in respiratory, skin as well as digestive problems.

Many biochemical or chemical technologies have been applied to reduce THM formation potential (THMFP) and for degradation of THMs as well as THM precursors. Zainudina et al. (2018) indicated advanced oxidation processes (AOPs) might be beneficial for degrading THMs, THM precursors, and for reduction of THMFP. AOPs represents technologies that generate reactive intermediates, such as the hydroxyl radical (·OH) for degradation of contaminants. This study intends to compare two AOPs on removal of THMs and THMFP: UVC (254 nm) irradiation

combined with free chlorine (UVC/Cl_2) and combined vaccum-ultraviolet (185 nm)/ UVC (254 nm)/ chlorine (VUV/UVC/Cl_2). The former method has been proven to efficiently remove THM precursors, THMs and THMFP (Hansen et al., 2013). However, there is a knowledge gap that a limited number of studies have been done previously to examine the effects of VUV radiation on THMFP and THMs (Buchanan et al., 2006).

Additionally, a VUV/UVC absorption spectra (180-300 nm) was measured for aqueous solutions of THMs to aid in interpretation of experiments involving direct photolysis by UVC/VUV irradiation. Then, the degradation kinetics of pure THM species and chloramines resulting from UVC irradiation, VUV/UVC irradiation, and both irradiation methods combined with chlorination were explored.

The experiments involved the use of a mini-fluidic VUV/UVC photoreaction system combined with membrane introduction mass spectrometry (MVPS-MIMS). The MVPS-MFPS employed a low-pressure Hg lamp as the source of VUV and UVC radiation. Two quartz capillary transmission tubes were included to allow UVC exposure. One of the tubes was made of a grade of quartz that allowed VUV and UVC to be transmitted, while the second quartz tube was essentially opaque to VUV radiation. Data collected by MIMS allowed reaction progress for aqueous solutions of each of the seven volatile DBPs. As compared with conventional analysis methods, such as GC-MS, MIMS provided important advantages, including the ability to monitor reaction progress in real time. Exposure of the target compounds to UVC or VUV/UVC irradiation was adjusted by changing the flow rates through the system.

LITERATURE REVIEW

Trihalomethanes (THMs) and Chloramines

The volatile DBPs investigated in this study included four common trihalomethanes (THM) and three inorganic chloramines, including chloroform ($CHCl_3$), dichlorobromomethane ($CHBrCl_2$), dibromochloromethane ($CHBr_2Cl$), bromoform ($CHBr_3$), monochloramine (NH_2Cl), dichloramine ($NHCl_2$) and trichloramine (NCl_3). The degradation of these seven compounds as a result of exposure to UVC irradiation (254 nm) and combination of VUV and UVC irradiation (185 nm and 254 nm) in MVPS were examined. Before addressing the responses of these compounds to UVC or VUV exposure, it is relevant to understand the formation of THMs and inorganic chloramines in the chlorinated water.

Since the first identification of THMs reported by J.J Rook in 1974, a large number of DBPs (>500) have been actively detected and investigated. Among these, the THMs represent up to 20% of the total concentration of chlorinated DBPs (Richardson, 2003). The chlorinated/brominated THMs (chloroform ($CHCl_3$), dichlorobromomethane ($CHBrCl_2$), dibromochloromethane ($CHBr_2Cl$), and bromoform ($CHBr_3$)), have been reported to commonly occur in the treated wastewater, treated drinking water, in water distribution systems, and in swimming pools (Ivannenko & Zogorski, 2006; Krasner et al., 1989; Krasner et al., 2009; Peng et al., 2016). As an examples, the THMs concentrations were found to be 57 µg/L and 2 µg/L in the well-nitrified and poorly-nitrified waste water, respectively (Krasner et al., 2009). Another study indicated total THM concentrations ranging from 46 to 279 µg/L in the post chlorinated wastewater effluents (Watson et al., 2012). In drinking water treatment, the previous median concentrations of THMs were reported to be 39

µg/L (Krasner et al., 1989). Panyakapo et al. (2008) reported that the concentrations of total THMs, chloroform, bromodichloromethane, dibromochloromethane and bromoform in water were 12.70–41.74, 6.72–29.19, 1.12–11.75, 0.63–3.55 and 0.08–3.40 µg/L, in respectively 60 tap water samples; corresponding concentration ranges in swimming pool water samples were 26.15–65.09, 9.50–36.97, 8.90–18.01, 5.19–22.78 and ND–6.56 µg/L, respectively (Panyakapo, Soontornchai, &Paopuree, 2008)

The formation of classical THMs was first studied based on the chlorination or chloramination of natural organic matter (NOM), with or without bromide (Rook, 1974). This reaction is a complex process influenced by many factors, such as reaction time, UVC_{254} absorption, pH, temperature, DOC concentration, bromide concentration, and chlorine dose. The relationships between those parameters and THMs formation have been investigated in many studies (Spiliotopoulou et al., 2015; Wang et al., 2010). NOM comprises a group of humic substances, carbohydrates, amino acids, proteins and carboxylic acids, each of which function differently as precursors to formation of THMs (Bond et al., 2012). Humic substance comprises a number of functional groups, including acetaldehyde, methyl ketones, ethanol, and secondary alcohol. One of important reaction that related to THM formation called “Haloform Reaction” is a common chemical reaction that generates haloforms by reacting hypohalous acids with methyl ketones in the presence of a base. The detailed pathway is displayed in Figure 1.

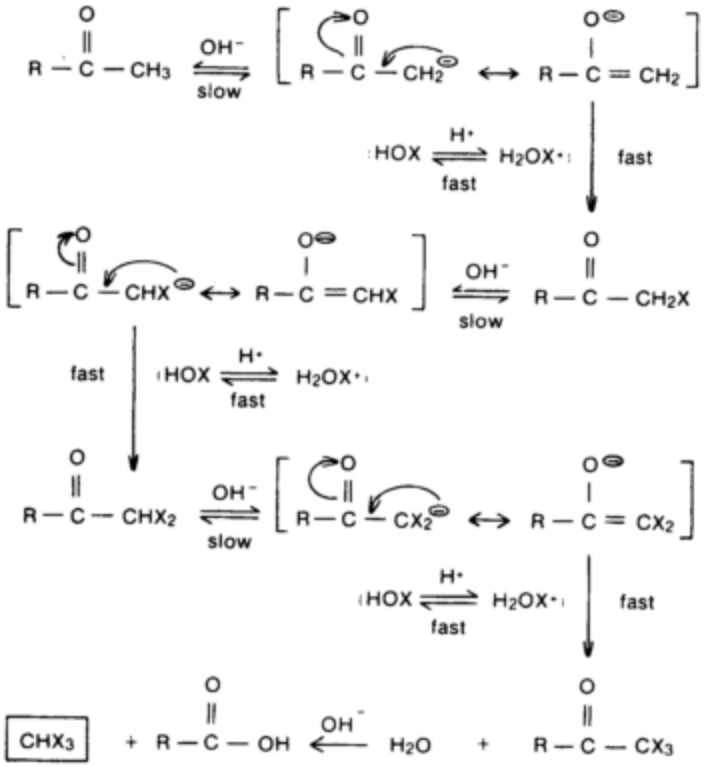

Figure 1 Haloform Reaction Pathway (Trussell & Umphres, 1978)

Reaction time is positively linked to total THM concentrations and THMFP. Chang et al. (1996) and Champagne (2008) pointed out most THMs were formed within the first 8 hours, often followed but a slow increase up to 48 hours.

Bromide, as an another important participant in THM formation, will also influence the THM formation rate and the THM yield (Trussell & Umphres, 1978). Bromide is present as 10-1000 µg/L in fresh water and at around 65 mg/L in seawater (WHO, 2009). In the presence of hypochlorous acid (HOCl), bromide is readily oxidized to hypobromous acid (HOBr) at neutral PH, shown in equation 1. Hypobromous acid (HOBr) will equilibrate with the hypobromite ion (OBr^-), with a pKa of roughly 8.7.

$$HOCl + Br^- \leftrightarrow HOBr + Cl^- (1)$$

HOBr will promote the formation of brominated-DBPs (dichlorobromomethane, dibromochloromethane, and bromoform).

Changes in chlorine and bromide concentration can alter THMs speciation. At a low concentration of bromide (<0.001 mg/L), chloroform tends to dominate total THMs (Chang et al., 1996). As concentration of bromide ion is increased, the THM distribution shifts toward the brominated forms (Symons et al., 1993).

THM concentration is increased with pH. It is indicated that chlorinated DBP was much more dependent upon pH than brominated DBP. The increase in chloroform concentration is 2.4 times more than increase in bromodichloromethane concentration within 72 hours (Hua & Reckhow, 2012).

Monochloramine (NH_2Cl) will occur in drinking water when it is used as a surrogate disinfectant in distribution system or when reduced nitrogen (often in the form of NH_3) is present. Chloramine disinfection will produce some disinfection byproducts including THMs but generates approximately two thirds of THMs formed by chlorine treatment (EPA, 1994). The remaining chloramines ($NHCl_2$ and NCl_3) are not usually present in drinking water but often occur in swimming pool. Chloramines have been found to be more stable than free chlorine, and they are important precursors for the formation of nitrogenous disinfection byproducts (Sakai et al., 2016). The formation of chloramines is influenced by contact time, pH and chlorine to ammonia molar ratio (Jafvert & Valentine, 1992).

$$NH_3 + HOCl \leftrightarrow NH_2Cl + H_2O \quad (2)$$

$$NH_2Cl + HOCl \leftrightarrow NHCl_2 + H_2O \quad (3)$$

$$NHCl_2 + HOCl \leftrightarrow NCl_3 + H_2O \quad (4)$$

Toxicity and Regulation

Although chlorination has been used for water treatment for a long time, the first identification of THMs was in 1974 (Rook, 1974). The US Environmental Protection Agency (EPA) implemented regulations for DBPs in the amendments to the Safe Drinking Water Act (SDWA) in 1986 and cooperated with the Association of Metropolitan Water Agencies (AMWA) to start a study of DBPs occurrence and concentrations.

The maximum contaminant level (MCL) of total THMs (sum of chloroform, dichlorobromomethane, dibromochloromethane, and bromoform) was regulated to be 80 µg/L by the EPA in the Safe Drinking Water Act (SDWA). The World Health Organization (WHO) has provided recommendations for the maximum acceptable concentrations of chloroform, dichlorobromomethane, dibromochloromethane, and bromoform to be below 200, 60, 100, and 100 µg/L, respectively. The limit of total THMs has been regulated to be below 100 µg/L by European Union (EU) standards. The Maximum Residual Disinfectant Level (MRDL) of chloramines (monochloramine, dichloramine, and trichloramine) is 4 mg/L according to the National Primary Drinking Water Regulations (NPDWR, US EPA).

Table 1 Regulations on THMs (Richardson, 2003)

US EPA Regulations	
DBP	MCL (mg/L)
Total THMs	0.080
5 Haloacetic acids	0.060
Bromate	0.010
Chlorite	1.0
World Health Organization (WHO) Guidelines	
DBP	Guideline value (µg/L)
Chloroform	200
Bromodichloromethane	60
Dibromochloromethane	100
Bromoform	100
Dichloroacetic acid	50[b]
Trichloroacetic acid	100[b]
Bromate	25[b]
Chlorite	200[b]
Chloral hydrate (trichloroacetaldehyde)	10[b]
Dichloroacetonitrile	90[b]
Dibromoacetonitrile	100[b]
Trichloroacetonitrile	1[b]
Cyanogen chloride (as CN)	70
2,4,6-Trichlorophenol	200
Formaldehyde	900
European Union (EU) Standards	
DBP	Standard value (µg/L)
Total THMs	100
Bromate	10[c]

Based on EPA guidelines, both chloroform ($CHCl_3$) and dichlorobromomethane ($CHBrCl_2$) have been identified as reasonably anticipated human carcinogens; the remaining two THMs (dibromochloromethane ($CHClBr_2$), and bromoform($CHBr_3$)) have been described as probable carcinogens. Exposure to THMs has been noted to increase risk of rectal, bladder, and colon cancer (Boorman et al., 1999; Villanueva et al., 2006). Watson et al. (2012) studied the toxicity of THMs in chlorinated wastewater by using a series of bioassays and concluded that THMs were toxic and

harmful to aquatic organisms. Also, long-term exposure to a low concentrations of THMs has been associated with adverse reproductive effects on people that resulted in low birth weight births, preterm births and gestational age births (Kumar et al., 2014).

Chloramines can irritate the skin, eyes, the nose, throat and lungs. Although some clinical reports present some cases of skin problems due to exposure to monochloramine related to drinking water use, there is no sufficient clinical and epidemiology reports in animals or humans to reveal associations between monochloramine that meets regulations in drinking water and adverse health effects, including skin problems, respiratory problems, digestive problems and cancer (Department of Health Vermont, 2012; EPA, 1992, 1994). The WHO elucidates that 0.25 to 0.3 mg/L monochloramine has been reported to induce acute hemolytic anemia, methemoglobinemia and hemolysis in hemodialysis individuals via dialysis (WHO, 2004). In addition, exposure to trichloramine (NCl_3) has been linked to respiratory diseases including asthma especially in the swimming pool (Jacobs et al., 2007). (Oppenländer & Schwarzwälder, 2002)

Mechanism of UVC/Cl_2 and VUV/UVC/Cl_2

It is noted that two primary lines observed in the emission spectrum of low-pressure mercury lamp are at 185 and 254 nm, thus ultraviolet (UVC) refers to radiation at 254 nm and Vacuum-UVC (VUV) represents the radiation at 185 nm in this study. In addition, the emission intensity of VUV is reported to be 8% of UVC output (Table 2). Advanced oxidation processes (AOPs), as technologies that involve production of strong oxidants as reactive intermediates, such as the hydroxyl radical (·OH), are used commonly for degrading organic pollutants in water. Some AOPs utilize UV radiation. Both UVC irradiation with chlorine (UVC/Cl_2) and VUV irradiation

combined with UVC/Cl_2 (VUV/UVC/Cl_2) are advanced oxidation processes (Jin et al., 2011; Li et al., 2016).

Table 2 Emission intensity of low-pressure mercury lamp relative to output at 254 nm (Masschelein & Rice, 2002)

λ (nm)	Emitted intensity ($I_{o,\ rel}$)
184.9	8
296.7	0.2
248.2	0.01
253.7	100
265.2–265.5	0.05
275.3	0.03
280.4	0.02
289.4	0.04
405.5–407.8	0.39
302.2–302.8	0.06
312.6–313.2	0.6
334.1	0.03
365.0–366.3	0.54

Mechanism of UVC/Cl_2

The UVC/Cl_2 process is water treatment process, not only inactivation of microbial pathogens but also for oxidation of organic pollutants in drinking water; it may also be beneficial in terms of DBP degradation (Judd & Jeffrey, 1995). The UVC/Cl_2 process is initiated by photolysis of free chlorine to yield the chlorine radical (·Cl) as the hydroxyl radical (·OH) through equation 5 to 8.

$$HOCl \leftrightarrow H^+ + OCl^- \quad (5)$$

$$HOCl + hv_{254} \leftrightarrow \cdot OH + Cl \cdot \quad (6)$$

$$OCl^- + hv_{254} \leftrightarrow \cdot O^- + Cl \cdot \quad (7)$$

$$O^- + H_2O \leftrightarrow \cdot OH + OH^- \quad (8)$$

Mechanism of VUV/UVC/Cl_2

VUV irradiation can be considered as an AOP since water can be photolyzed by VUV radiation to form reactive oxidants, including ·OH, the hydrogen radical (H·) and the hydrated electron (e_{aq}^-) through equation 9 to 10. The homolysis of water is the major reaction (equation 9), and ionization reaction is the minor path (equation 10). The formation efficiency of ·OH and H· are higher than $e_{aq.}^-$ The quantum yields for homolysis and ionization are 0.33 and 0.045, respectively; thus the total quantum yield (sum of quantum yields of homolysis and ionization) of water irradiated by VUV radiation is 0.375 (Gonzalez et al., 2004; Li et al., 2016).

$$H_2O \xrightarrow{hv\ 185nm} \cdot OH + H^{\cdot} \qquad (9)$$

$$H_2O \xrightarrow{hv\ 185nm} \cdot OH + H^+ + e_{aq}^- \qquad (10)$$

·OH, H· and e_{aq}^- tend to induce secondary reactions for the formation of more stable forms. It has been reported that H_2O_2 and H_2 are produced resulting from the self-combination of VUV-induced hydroxyl radicals and hydrogen radicals. Also, ·OH will combine with e_{aq}^- to form hydroxide (OH^-) which leads to increase pH.

$$\cdot OH + e_{aq}^- \rightarrow OH^- \qquad (11)$$

$$\cdot OH + \cdot OH \rightarrow H_2O_2 \qquad (12)$$

$$H^{\cdot} + H^{\cdot} \rightarrow H_2 \qquad (13)$$

It was indicated that Cl_2 was consumed faster in VUV/UVC/Cl_2 process than in UVC/Cl_2 process; more secondary radicals (·OCl), weaker oxidant agents, were formed to take the place of H_2O_2, and H_2O_2 formation may be inhibited by depletion of available Cl_2 (Li et al., 2016).

$$\cdot OH + HOCl \rightarrow \cdot OCl + H_2O \qquad (14)$$

$$\cdot OH + OCl^{-} \rightarrow \cdot OCl + OH^{-} \quad (15)$$

In addition, VUV radiation leads to direct photolysis of methanol (equations 15 to 18) as well as oxidation (equations 19 and 20) by hydroxyl radical of methanol in aqueous systems (Gonzalez et al., 2004). Thus, methanol is regarded as a potential scavenger of hydroxyl radicals, which inhibits the effects of VUV radiation on removal of micropollutants.

$$CH_3OH \xrightarrow{hv\ 185nm} CH_3O^{\cdot} + H^{\cdot} \quad (16)$$

$$CH_3OH \xrightarrow{hv\ 185nm} {}^{\cdot}CH_2OH + H^{\cdot} \quad (17)$$

$$CH_3OH \xrightarrow{hv\ 185nm} CH_3 + HO^{\cdot} \quad (18)$$

$$CH_3OH \xrightarrow{hv\ 185nm} CH_2O + H_2 \quad (19)$$

$$CH_3OH + HO^{\cdot} \rightarrow {}^{\cdot}CH_2OH + H_2O \quad (20)$$

$$CH_3OH + HO^{\cdot} \rightarrow CH_2O \cdot + H_2O \quad (21)$$

Removal of THMs by UVC and VUV combined with other treatment

Lamsal et al. (2011) and Rudra et al. (2005) indicated UVC irradiation alone and H_2O_2/UVC can decrease THMFP and production of THMs, and UVC/O_3 allowed reductions in THMFP and THM precursors.

Although VUV-induced photolysis of water yields hydroxyl radicals and is found to be useful for the removal of micropollutants, few studies have addressed the effects of VUV irradiation on THMs, THMFP and THM precursors (Li et al., 2016; Zoschke et al., 2014). VUV irradiation has been found to oxidize NOM more effectively than UVC irradiation and H_2O_2/UVC/VUV

treatment was demonstrated to remove more NOM due to more hydroxyl radicals being involved in the reaction (Thomson et al., 2002). Buchanan et al (2006) found significant reductions in THMFP and $CHCl_3$, $CHBrCl_2$ and $CHClBr_2$ in VUV and UVC treatment at a high UVC dose (> 40 J cm^{-2}), and differences in removal efficiency of between VUV treatment and UVC treatment extended with an increasing dosage. The study reported by Buchanan et al (2006) was performed at a UVC dose ranging from 16-233 J cm^{-2} and a high level of chlorine at 40 mg/L. Buchanan et al. (2008) indicated that VUV combined with biologically activated carbon (BAC) could decrease THMFP by 60-70% and DOC concentration by 54%.

MATERIAL AND METHODS

Experimental Set-up

A mini-fluidic VUV/UVC photoreaction system developed by Li et al. (2016) was connected with membrane introduction mass spectrometry (MVPS-MIMS) system to explore the degradation kinetics of single DBPs in aqueous solutions based on exposure to UVC, UVC/Cl_2, VUV/UVC and VUV/UVC/Cl_2 processes. Time-course changes in the concentrations of THMs, total THMs and THMFP resulting from chlorination of NOM with the presence of bromide with UVC irradiation or combined VUV/UVC irradiation. In the MVPS, a 8 W cold-cathode low-pressure mercury lamp covered with synthetic quartz (Suprasil quartz) is installed at the centerline of the device, which can emit UV and VUV radiation (Zoschke et al., 2014). According to the emission intensity of low-pressure mercury lamp, VUV emission takes up to 8% of the total output (Zoschke et al., 2014). In addition, a synthetic quartz VUV/UVC tube that had high transmittance for both VUV (185 nm) and UVC (254 nm) radiation, along with a Ti-doped quartz tube that only received UVC radiation, were positioned parallel to the lamp at a radial distance of 5 mm from the lamp surface. Both tubes had an inner diameter of 3 mm and a length of 297 mm. Because these transmission tubes had otherwise identical physical characteristics, the UVC fluence delivered to fluid flowing at a fixed flow rate through each tube was expected to be identical for the UVC and VUV/UVC paths; this assumption was confirmed previously (Li et al., 2016). The MIMS system was employed with 6850 GC system and 5975C mass spectrometer with triple-axis detector. Volatile DBPs can be quickly quantified via selective ion monitoring (SIM).

Actinometry

Measurement of the direct fluence rate of received by solutions flowing through the VUV/UVC tubes in the MVPS is accomplished more easily by chemical actinometry than by radiometry due to geometric constraints of the radiometer detector and inability of the conventional radiometer to measure VUV radiation. Uridine and methanol were chosen as actinometers to determine the UVC and VUV fluence (Heit et al., 1998; Jin et al., 2007). Since the VUV/UVC tube absorbs both UVC and VUV radiation, the actual fluence received by fluid in the VUV/UVC tube ($F_{VUV/UVC}$) is the sum of UVC fluence (F_{UVC}) and VUV fluence (F_{VUV}) (Li et al., 2016). The exposure time was approximated by the mean hydraulic detention time in the tube:

$$t = \frac{\pi r^2 h}{v} \quad (22)$$

$$F_{VUV/UV} = F_{VUV} + F_{UV} \quad (23)$$

where r and h are the radius and length of UVC or VUV/UVC tubes (cm); v represents the average flow rate (mL/s); t is the exposure time (s).

UVC Fluence Measurement

A 200 mL sample of a solution of 0.012 mM uridine (Sigma, St. Louis) was prepared with 1 mM phosphate buffer as the actinometer to measure the UVC photon fluence rate as a function of exposure time (Scholes et al., 1992). Uridine samples were collected by pumping uridine solution through the UVC tube to receive the irradiance at flow rates of 5.1, 4.2, 3.0 and 2.4 mL/min respectively. All irradiated samples as well as unirradiated 0.012 mM uridine solution were scanned by the Agilent Cary 6000i UVC-Vis-NIR Spectrophotometer at a range of 200-300 nm. It was noted that uridine degradation by UVC photolysis followed the first order kinetics, and

absorbance of uridine was small (Scholes et al., 1992; Zhang et al., 1997). The degradation rate constant k can be expressed as equation 24 according to first order kinetics and photoreaction of uridine.

$$k = 2.303 \times 1000 \times \frac{E}{U} \times \varepsilon \times \Phi = \frac{\ln(C/Co)}{t} \quad (24)$$

Where E is incident fluence rate (mW cm^{-2}); U is the photon energy observed at 254 nm and was calculated to be 4.71×10^{8} mJ $Einstein^{-1}$. Because only monochromatic radiation was observed in UVC tube, the molar absorption coefficient of 0.012 mM uridine solution at 254 nm (ϵ_{254}) was used. The quantum yield of uridine (Φ) was assumed to be 0.020 mol $Einstein^{-1}$ (S. Jin et al., 2007). Co and C are the concentration of actinometer before and after UVC irradiation (mM). t is the exposure time (s).

Based on the Beer-Lambert Law, ln(Co/C) is equal with ln (A°_{262}/A_{262}). A°_{262} and A_{262} are the absorbance of uridine solution without and with irradiation, respectively.

$$\frac{\ln(Co/C)}{t} = \frac{\ln(\frac{A^{\circ}_{262}}{A_{262}})}{t} \quad (25)$$

UVC fluence [H (mJ cm^{-2})] is the product of fluence rate (E) and exposure time (t).

$$H = E \times t = \frac{E}{U} \times t \times U \quad (26)$$

Combine and rearrange the equation 24, 25 and 26 to get equation 27 (S. Jin et al., 2007).

$$H = \frac{\ln(\frac{A^{\circ}_{262}}{A_{262}}) \times U}{2.303 \times 1000 \times \epsilon_{\lambda} \times \Phi} \quad (27)$$

VUV/UVC Fluence Measurement

The VUV/UVC tube is a quartz tube that receives a combination of VUV and UVC exposure (185 nm and 254 nm). The uridine actinometer used in the UVC tube is unable to perform well since this kind of actinometer receives both UVC and VUV exposure; in another words, it was anticipated that uridine would undergo significant decay by UVC photolysis as well as the hydroxyl radical oxidation and insignificant VUV photolysis induced decay (Li et al., 2016).

It has been reported that hydroxyl radical induced degradation of methanol can be used as an actinometer for VUV (185 nm) radiation aqueous samples (Heit et al., 1998). Reactions of VUV-induced water/methanol solutions involve photolysis of methanol, photolysis of water (the production of hydroxyl radicals, hydrogen radicals and hydrates electrons) and a series of subsequent secondary reactions which alter the concentrations of methanol and hydroxyl radicals. The decay of methanol results from the direct VUV photolysis and the hydroxyl radical oxidation; the latter degradation is primary. It has been established that hydroxyl radical induced degradation of methanol dominates in total decay when methanol concentration ranges from 75 to 250 mM, and it follows the zero-order kinetics. The decay of methanol can be expressed as below.

$$\frac{-d[MeOH]}{dt} = 0.946(\Phi_{MeOH} f_{MeOH} + \Phi_{H2O} f_{H2O}) \times \frac{q}{V} = k_{MeOH} \quad (28)$$

q represents the absorbed photon flux (Einstein s^{-1}); k_{MeOH} is the slope of decay of methanol (M s^{-1}); V represents the volume irradiated methanol solution (L). The total quantum yield of methanol ($\Phi_{MeOH} = 1$ mol $Einstein^{-1}$) is the sum of quantum yield of all photoreactions of methanol by VUV irradiation (Buenker et al.,1984). The total quantum yield of water ($\Phi_{H2O} = 0.375$ mol $Einstein^{-1}$) involves quantum yield of homolysis and ionization of water by VUV irradiation (Heit et al., 1998). The production of methanol by the disproportionation reaction of hydroxymethyl

radicals resulting from subsequent radical reactions has been reported to be 5.4% of total reduced methanol, thus a factor of 0.946 represents the fraction of methanol degraded by hydroxyl radicals (Heit et al., 1998; Oppenländer & Schwarzwälder, 2002). The incident photon fractions absorbed by methanol and water (f_{MeOH} and f_{H2O}) used in this study were assumed to be 0.0038 and 0.9962 (equations 29 and 30), respectively (Li et al., 2016).

$$f_{MeOH} = \varepsilon_{185,MeOH}[MeOH]/(\varepsilon_{185,MeOH}[MeOH] + \varepsilon_{185,H2O}[H_2O]) \quad (29)$$

$$f_{H_2O} = \varepsilon_{185,H2O}[H_2O]/(\varepsilon_{185,MeOH}[MeOH] + \varepsilon_{185,H2O}[H_2O]) \quad (30)$$

[MeOH] and [H_2O] are the initial concentration of methanol and water (M); $\varepsilon_{185,MeOH}$ and $\varepsilon_{185,H2O}$ are molar absorption coefficient of methanol and water at 185 nm (M^{-1} cm^{-1}).

VUV fluence rate is equal to the absorbed photon flux (q) multiplied by photon energy (U) and divided by cross section area of VUV/UVC tube. The VUV fluence can be calculated with equation 31 (Li et al., 2016; Oppenländer & Schwarzwälder, 2002).

$$FR_{VUV} = \frac{qU}{A} = \frac{k_{MeOH}VU}{0.946(\Phi_{MeOH}f_{MeOH}+\Phi_{H2O}f_{H2O})A} \quad (31)$$

FR_{VUV} represents the VUV fluence rate at 185 nm (mW cm^{-2}); U is the photon energy at 185 nm (mJ $Einstein^{-1}$); A is the cross-section area of VUV/UVC tube (cm^2).

Methanol concentration in aqueous solutions can be quantified by a number of methods, including HPLC, GC-MS or GC-FID, FT-IR and an enzymatic method (Xu et al., 2012; Zhang et al., 2015). However, the analytical equipment needed to conduct these measurements was not available for this study. Therefore, a colorimetric method was used to determine the concentration of methanol

in the simple water matrix. Specifically, the method involving Chromotropic Acid (CA), which is used to determine the formaldehyde generated from the oxidation of methanol by potassium permanganate; this method was recommended by the National Institute for Occupational Safety and Health (NIOSH) and Association of Official Analytical Chemists (AOAC) (Boos, 1948; Horwitz & Latimer, 2005; NIOSH, 1994).

The CA Method was applied to measure the methanol content in water (Resolution Oeno, 2009). One drop of 50% (m/v) phosphoric acid solution and two drops of 5% (m/v) potassium permanganate solution were added to the samples and the control in vials, then allowed to stand for 10 min. Solutions were spiked with four drops of freshly prepared 2% (m/v) sodium sulfite solution which causes decolorization of the remaining potassium permanganate. 5 mL 0.05% (m/v) CA in 75% (v/v) concentrated sulfuric acid solution was added to the vials. The vials were placed in a 70°C water bath for 20 min; then absorbance at 570 nm was measured using a UVC-Vis

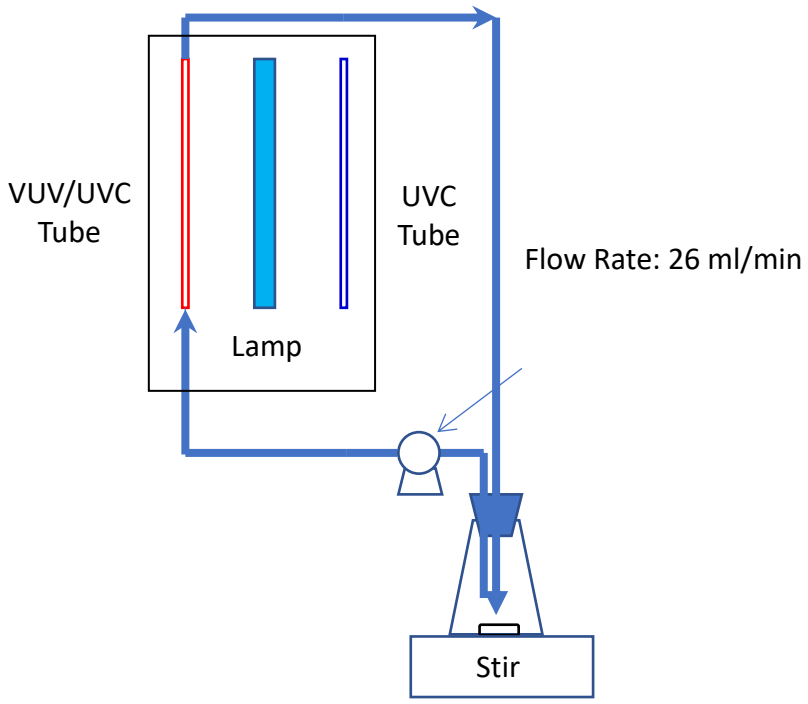

Figure 2 Schematic illustration of methanol samples collection for VUV fluence measurement.

spectrometer; the methanol concentration was calculated by comparison of the colorimetric reading with those of a standard curve, which was developed form a series of aqueous solutions with known concentrations of methanol.

The standard curve was prepared at concentrations of 25, 50, 100, 150, 200 and 250 mg/L methanol. A 20 mL 95 mM methanol was continuously pumped through VUV tubes at a flow rate of 26 mL/min as Figure 2 shows. The flow rate was anticipated to be large enough to ignore passing time wasted in connections, thus reaction time was assumed to be equal with irradiation time. 0.5 mL solutions were collected at given reaction time of 5.30, 16.25, 27.00 and 31.00 min and diluted to 7.5 mL with NANO water. Each 0.5 mL diluted solution was used to be measured.

Haloform Absorption Spectra

Aqueous solutions of individual haloforms were prepared from the ACS Reagent grade chemicals and oxygen-free water that prepared from degassed HPLC-grade water in a MBRAUN glove box workstation. Oxygen was purged from the water (solvent) because it strongly absorbs VUV radiation. Nitrogen gas (>99%) was used to purge the oxygen from water. Chloroform ($CHCl_3$), dichlorobromomethane ($CHBrCl_2$), dibromochloromethane ($CHBr_2Cl$), and bromoform ($CHBr_3$) were diluted to the target concentration with oxygen-free water in 300 mL BOD bottles. The bottles were filled and capped in the glove box with a nitrogen atmosphere to prevent inclusion of dissolved oxygen. No head space or air bubbles were allowed in the bottles.

The well-mixed samples were immediately transported to the Brown Laboratory of Chemistry at Purdue University and scanned by the Agilent Cary 6000i UVC-Vis-NIR Spectrophotometer. The

sample space in the spectrophotometer was operated with a N_2 atmosphere. An absorbance scan (180-300 nm) was run on all samples, as well as oxygen-free water and a blank cuvette filled with N_2. To account for absorbance by non-target factors of the system, including water and the cuvette, three experiments were processed: (1) A blank cuvette filled with N_2 was placed in the sample cell and empty reference cell was set. The result was the absorbance of cuvette. (2) A cuvette filled with oxygen-free water was placed in the sample cell and a blank cuvette filled with N_2 was placed in the reference cell. This approach was used to measure the absorbance of water. (3) Oxygen-free water was regarded as reference (or baseline) and four haloforms were put in the sample cell, respectively. This primary experiment was applied to obtain haloforms spectra.

Because the absorbance of water using 1 cm quartz cuvette was observed to be larger than 2, that exceeded the detection range. In order to reduce the measured absorbance of solvent, 1 mm standard rectangular spectrosil quartz cuvettes with a stopper (Starna Cells, Inc.) were used. The concentration of each haloform in solution was measured by the MIMS system. The molar absorption coefficients of haloforms were calculated based on the Beer-Lambert Law.

$$A = \varepsilon bc \qquad (32)$$

Where A represents the absorbance; b represents the path length; ε represents the molar absorption coefficient and c represents the molar concentration of the absorbing compound in solution.

Degradation Kinetics of DBPs in MVPS-MIMS System

The MVPS, introduced in Li et al. (2016), was developed to provide a method of UVC and VUV exposure; this method is particularly relevant for volatile compounds because the system provides little, if any opportunity for gas: liquid transfer.

The MIMS system was connected to the MVPS via a Teflon tee connector, which allowed diversion of excess flow from the MVPS (Figure 3). The optimal sample flow rate for the MIMS system has been estimated to be 0.7 mL/min; the flow rate delivered to the MVPS was controlled via pump 1 (Shang & Blatchley, 1999). Exposure time in this study was defined as the time that solution passed through UVC or VUV tubes and had a significant linear correlation with the flow rate in term of same volume of tubes.

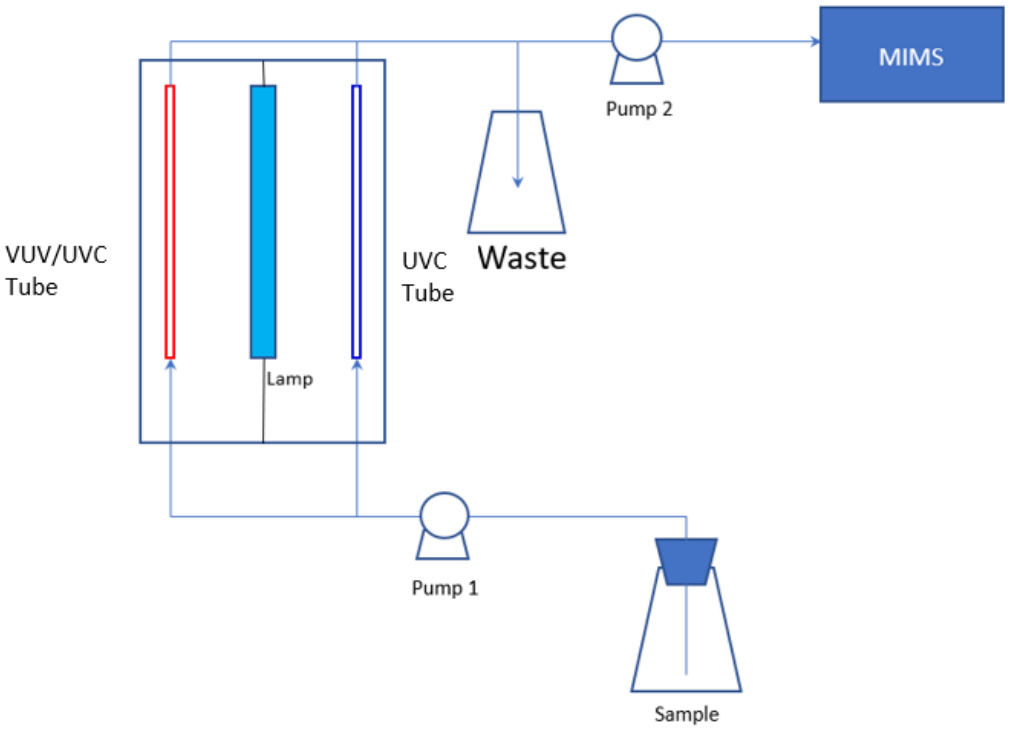

Figure 3 Schematic illustration of MVPS-MIMS system used to quantify DBP degradation resulting from UVC-associated treatment processes. Operating conditions: Free chlorine concentration = 67 μM (as Cl_2); THM concentration = 0.3 mg/L; Chloramine concentration = 5 mg/L; pH = 7 with 1 mM phosphate buffer.

The THM compounds ($CHCl_3$, $CHBrCl_2$, $CHBr_2Cl$, $CHBr_3$) were purchased from Sigma Aldrich (St. Louis). Pure THMs were dissolved in methanol and then diluted to target concentration (0.3 mg/L) with Barnstead NANO pure deionized water. Methanol can be irradiated by VUV radiation through equation 16 to 19, but indeed almost energy will be absorbed by water when concentration

of methanol (about 5 mM) is low in this study (Oppenländer & Schwarzwälder, 2002). All diluted solutions were controlled to pH 7 with a phosphate buffer. Remaining volatile DBPs ($NHCl_2$, NH_2Cl, NCl_3) were freshly prepared based on the reaction of regent grade sodium hydrochlorite (NaOCl) and ammonium chloride (NH_4Cl) as described by Shang & Blatchley (1999). 1 mM phosphate buffer was used to control the pH of NaOCl and NH_4Cl solutions. Monochloramine (NH_2Cl) was prepared at a chlorine to ammonia molar ratio of 1:1.03 at pH 10; dichloramine ($NHCl_2$) was prepared at a chlorine to ammonia ratio of 1.8:1 at pH 5 and allowed to stand overnight to complete the reaction; trichloramine (NCl_3) was prepared at a chlorine to ammonia ratio of 3.15:1 in a 35 °C water bath for 2 hours. The concentrations of the inorganic chloramines were determined via the DPD/KI colorimetric method (APHA, AWWA, & WEF, 1998).

The central goal of these experiments was to investigate the degradation kinetics and mechanism of DBP behavior in solutions subjected to a range of treatment processes including chlorination, chlorine, UVC, UVC/chorine, UVC/VUV and UVC/VUV/Chlorine. Sodium hypochlorite (NaOCl), as free chlorine, was spiked to reach an initial free chlorine concentration of 0.07 mM as Cl_2. All solutions were pumped at flow rates ranging from 5 to 2 mL/min through MVPS; flow diversion (described above) was used to introduce liquid samples to the MIMS at the optimal flow rate of 0.7 mL/min. As first-order degradation kinetics of THMs by UVC irradiation has been reported in other studies, a function of ln (C/C_o) with time is anticipated (Hansen et al., 2013). The control experiment will be conducted that all samples were pumped at identical flow rates as before without UVC/VUV irradiation.

THM Formation

After degradation kinetics rates of pure THMs were investigated in the MVPS-MIMS system, a simulation of conditions that would lead to THM formation based on reactions of free chlorine with natural organic matter (NOM) in the presence of bromide was also examined. Humic Acid (Sigma Aldrich) is a main component of NOM to produce THMs; dissolved organic carbon (DOC) can be quantified by TOC-L. In total, three experiments were carried out: (a) humic acid solution (DOC =1.45 mg/L), 6.7 µM potassium bromide (KBr), 67 µM sodium hypochlorite (as free Cl_2), were buffered to pH 7 via phosphate buffer and spiked into a 100 mL sealed flask equipped with a stir bar, respectively. Freshly prepared samples were mixed for 1 min and immediately pumped into a MVPS-MIMS system at a flow rate of 3 mL/min and formed THMs, THM species and THMFP after an exposure to UVC or VUV/UVC radiation was researched. (b) Similar with the

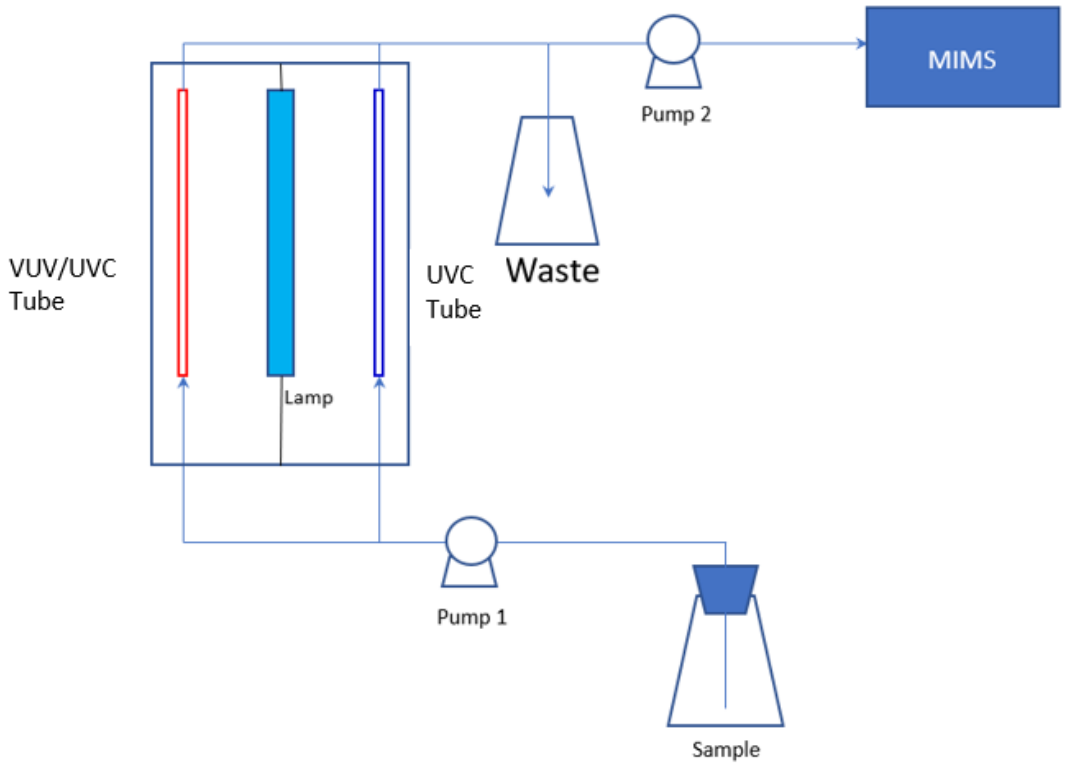

Figure 4 A schematic for experiment (a). Initial condition: DOC=1.25 mg/L; Cl_2 = 67 µM; Br^-=6.7 µM; pH=7; T=23 °C.

experiment (a), humic acid, potassium bromide and free chlorine were mixing together for 1 min and instantly pumped into the MVPS to receive the UV or VUV radiation. In contrast to the experiment (a) that subsequently pumped solution to MIMS, next step in this experiment was to collect irradiated samples in 40 mL vials with no headspace and THMs were determined after a

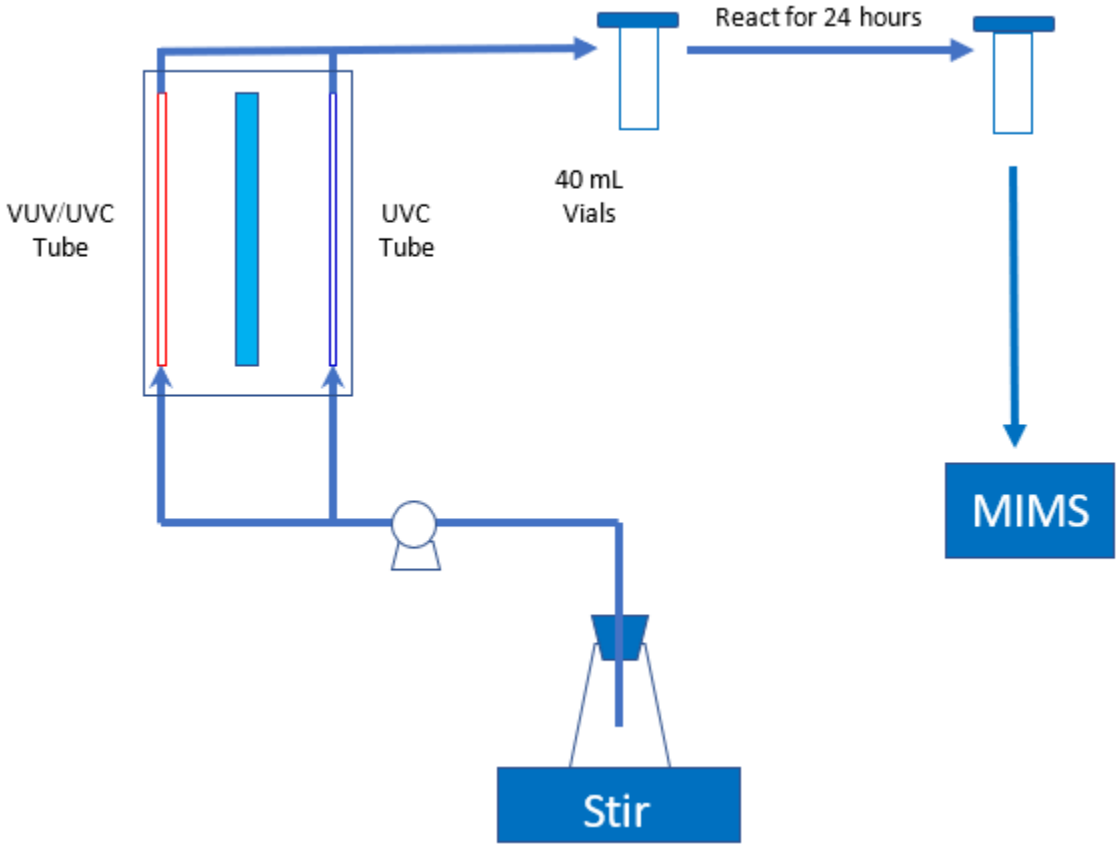

Figure 6 A schematic for experiment (b). Initial condition: DOC=1.25 mg/L; Cl_2 =67 µM; Br^- =6.7 µM; pH=7; T=23 °C.

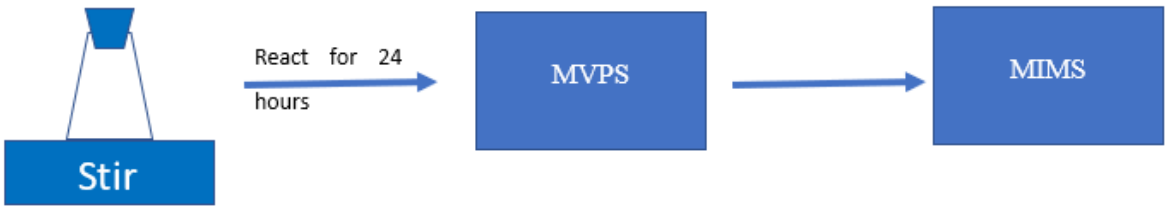

Figure 5 A schematic for experiment (c). Initial condition: DOC=1.25 mg/L; Cl_2 = 67 µM; Br^- =6.7 µM; pH=7; T=23 °C. After 24 hours, Cl_2 is not detectable.

24-hrincubation in the dark condition. (c) The same concentrations of humic acid, sodium hypochlorite as well as potassium bromide as described in former experiments were mixed in a 1 L flask without headspace and incubated for 24 hours in the dark to finish reactions at first. After 24 hours, solutions were irradiated by UVC and VUV/UVC and then analyzed by MIMS. Figure 4 to 6 illustrates the experimental equipment installation for THM formation experiments. In the experiments, free chlorine is the last compound to be spiked. Once free chlorine is contact with bromide and humic acid, it will combine with humic acid to produce THMs and with bromide to hypobromous acid that subsequently yield brominated-THMs.

DBPs Analytical Methods

The quantitative determination of volatile DBPs ($CHCl_3$, $CHBrCl_2$, $CHBr_2Cl$, $CHBr_3$, $NHCl_2$, NH_2Cl, NCl_3) was conducted by MIMS (Shang & Blatchley, 1999). Each volatile DBP yields a mass spectrum with unique m/z ratios. Table 3 listed the m/z peaks of various DBPs in the MIMS analysis. The concentrations of $CHCl_3$, $CHBrCl_2$, $CHBr_2Cl$, $CHBr_3$, $NHCl_2$, NH_2Cl, NCl_3 were quantified based on their respective signal abundance readings at m/z 83, 118, 129, 173, 53, 89, and 88, respectively.

Table 3 Characteristic m/z peaks applied in MIMS analysis(Weaver, 2008)

m/z	53	83	88	89	118	129	173
Compounds	NH_2Cl	$CHCl_3$ $CHBrCl_2$	NCl_3	$NHCl_2$	$CHCl_3$	$CHBrCl_2$ $CHBr_2Cl$	$CHBr_2Cl$ $CHBr_3$

The day to day sensitivity of MIMS changes with time, thus chloroform was used as calibration standard. A chloroform standard curve was created weekly and used to adjust the calibration curves of other DBPs, based on the assumption that changes in the response of the system to chloroform

were representative of changes in response to other compounds. The concentration of DBPs are computed based on equation 33 and equation 34 in the MIMS analysis. The standard curve was developed with concentrations of 0.05, 0.10, 0.20, and 0.50 mg/L of THMs and of 0.50, 1.00, 2.00 and 5.00 mg/L of chloramines (Appendix). If two or more of the THMs were present in a sample, equations 35 through 40 were used to estimate their concentrations in solution (Weaver, 2008).

$$Concentraion = \frac{abundance\ at\ m/z}{calculated\ slope\ at\ m/z} \quad (33)$$

$$\frac{standard\ slope\ of\ DBPs}{standard\ slope\ of\ chloroform} = \frac{Calculated\ slope\ of\ DBPs}{New\ slope\ of\ chloroform} \quad (34)$$

$$CHCl_3\ Abundance\ (^m/_Z = 83) = \frac{CHCl_3\ standard\ slope\ (^m/_Z=83) \times CHCl_3\ Abundance\ (^m/_Z=118)}{CHCl_3\ standard\ slope\ (^m/_Z=118)} \quad (35)$$

$$CHBrCl_2\ Abundance\ (^m/_Z = 83) = Total\ Abundance\ (^m/_Z = 83) - CHCl_3\ Abundance\ (^m/_Z = 83) \quad (36)$$

$$CHBrCl_2\ Abundance\ (^m/_Z = 129) = \frac{CHBrCl_2\ standard\ slope\ (^m/_Z=129) \times CHBrCl_2\ Abundance\ (^m/_Z=83)}{CHBrCl_2\ standard\ slope\ (^m/_Z=83)} \quad (37)$$

$$CHBr_2Cl\ Abundance\ (^m/_Z = 129) = Total\ Abundance\ (^m/_Z = 129) - CHBrCl_2\ Abundance\ (^m/_Z = 129) \quad (38)$$

$$CHBr_2Cl\ Abundance\ (^m/_Z = 173) = \frac{CHBr_2Cl\ standard\ slope\ (^m/_Z=173) \times CHBr_2Cl\ Abundance\ (^m/_Z=129)}{CHBr_2Cl\ standard\ slope\ (^m/_Z=129)} \quad (39)$$

$$CHBr_3\ Abundance\ (^m/_Z = 173) = Total\ Abundance\ (^m/_Z = 173) - CHBr_2Cl\ Abundance\ (^m/_Z = 173) \quad (40)$$

RESULTS AND DISCUSSION

UVC Fluence Measurement

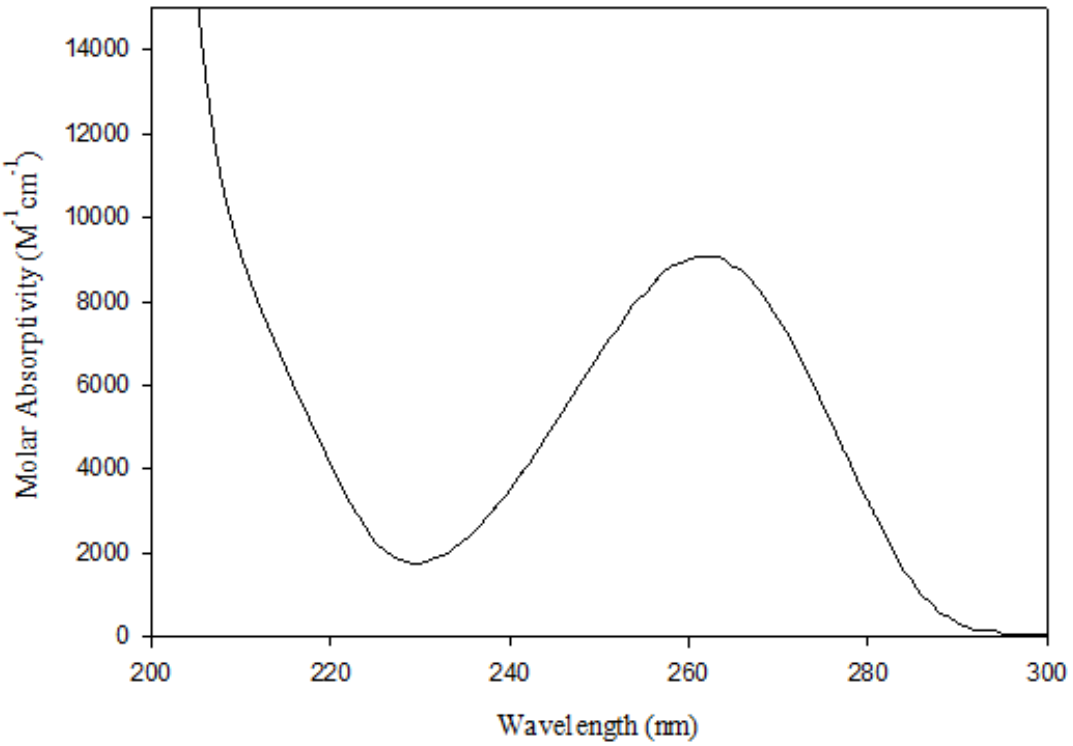

Figure 7 Molar absorption coefficient of 0.012 mM uridine solution with 10 mM phosphate buffer.

Figure 7 illustrates the molar absorption coefficient for uridine (in a 10 mM phosphate buffer) with controlled pH 7. Uridine displayed peak absorption at 262 nm; the molar absorption coefficient at 262 nm was 9083 M^{-1} cm^{-1}, which was less than value (10140 M^{-1} cm^{-1}) given in another study (Scholes et al., 1992). The molar absorption coefficient at 254 nm was determined to be 8000 M^{-1} cm^{-1}, which was smaller than the value (8775 M^{-1} cm^{-1}) reported before (Li et al., 2016). The product of molar absorptivity and quantum yield ($\varepsilon\Phi$) at 254 nm (160 L cm^{-1} $Einstein^{-1}$) was smaller than value (175 L cm^{-1} $Einstein^{-1}$) reported in Li et al., (2016).

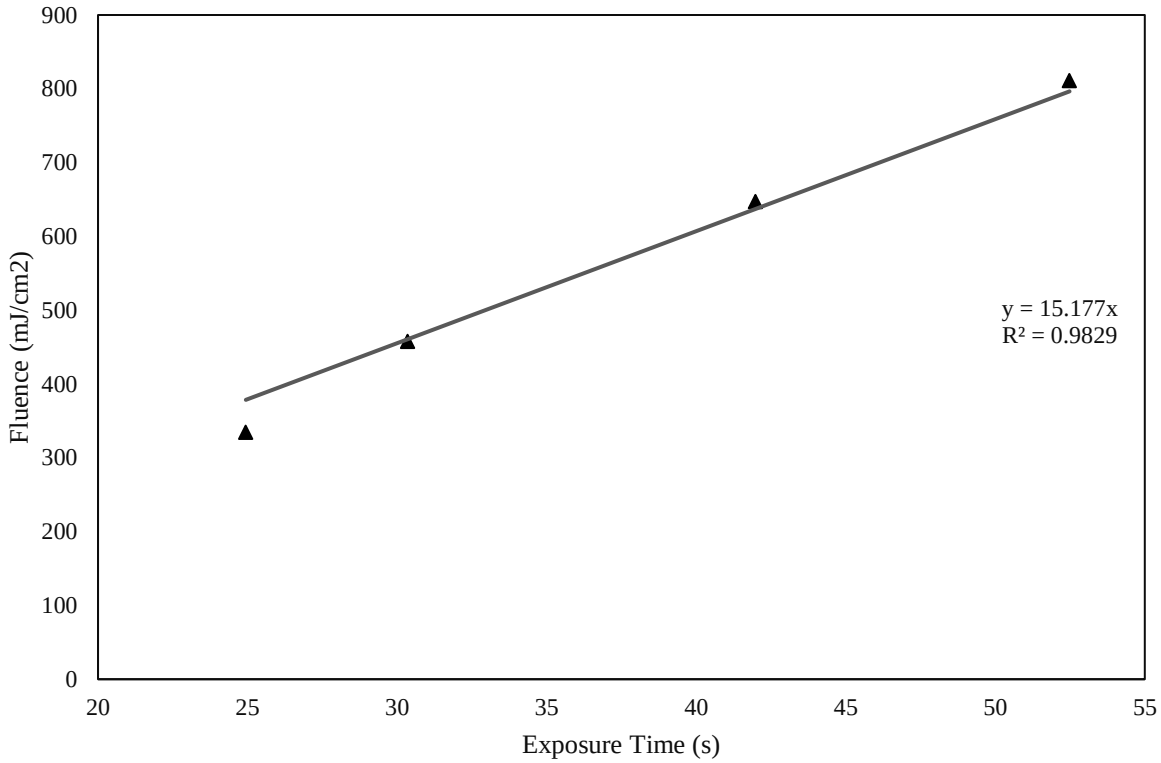

Figure 8 UVC Fluence as a function of exposure time as delivered by the MVPS reactor

Figure 8 illustrates the roughly linear dependence of (apparent) UVC dose delivered by the MVPS reactor as a function of (average) exposure time. For this calculation, the photoconversion of uridine was assumed to follow zero-order kinetics, because of the large value of optical density (at 254 nm) that characterized this solution in the reactor. The average UVC (254 nm) fluence rate delivered to the solution was the fluence divided by exposure time, which was equal to the slope (15.18 mW/cm^2 or 3.22×10^{-8} Einstein $cm^{-2}\,s^{-1}$).

VUV/UVC Fluence Measurement

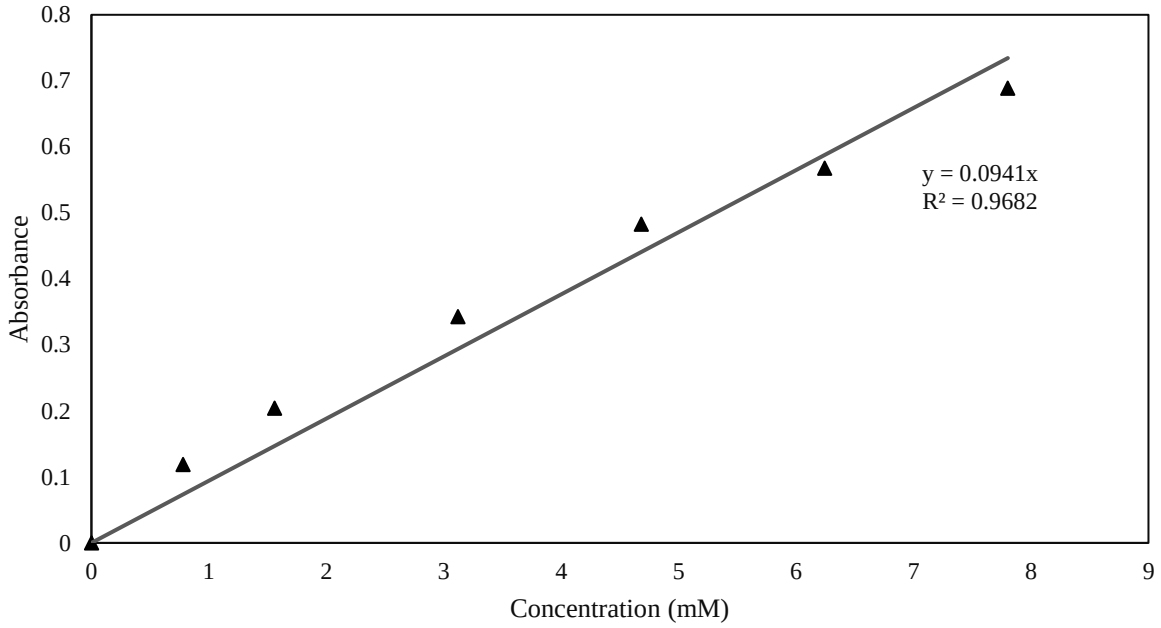

Figure 9 Methanol Calibration Curve

Figure 9 illustrates the absorbance of methanol samples with concentrations of 25, 50, 100, 150, 200 and 250 mg/L (0.78, 1.56, 3.12, 4.68, 6.24 and 7.80 mM) at 570 nm by using a UVC-Vis spectrometer. Those samples were prepared by CA method (described above). The regression line (solid line) shows roughly linear correlation between absorbance (at 570 nm) and concentration of methanol. The deviations between data points and regression line are random errors resulting from liquid delivery processes. Because CA method need to mix methanol with many chemicals to make samples, a little change of volume may lead to significant effects on results.

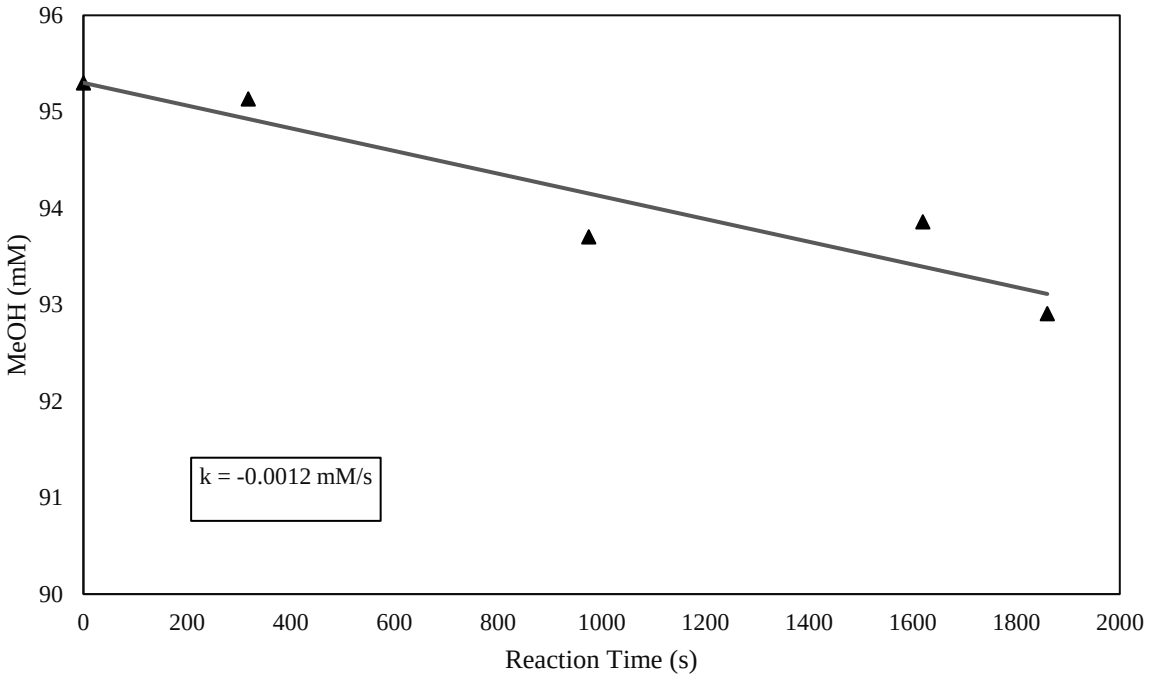

Figure 10 Hydroxyl radical induced degradation of methanol by VUV irradiation

Figure 10 presents the degradation of methanol by hydroxyl radical oxidation with time. X-axis is the reaction time (or irradiation time) and y-axis is the concentrations of each samples collected at 318, 975, 1620 and 1860 s. A methanol solution (95 mM) subjected to VUV irradiation and degraded following pseudo zero order kinetics, which was in agreement with trend described in Li et al. (2016) and Oppenländer & Schwarzwälder (2002). As shown in Figure 10, data points were not perfectly falling on the regression line; variations might be caused by inaccuracy of CA method and dilution process. The degradation slope of methanol was 0.0012 mM s^{-1}, thus VUV fluence rate was calculated as 4.75 mW cm^{-2} (or 0.73×10^{-8} Einstein cm^{-2} s^{-1}) based on the equation 31. Based on equation 23, the total fluence rate in VUV/UVC tube can be calculated by summing UVC fluence rate and VUV fluence rate at identical irradiation time (3.95×10^{-8} Einstein cm^{-2} s^{-1}).

Haloform Spectra

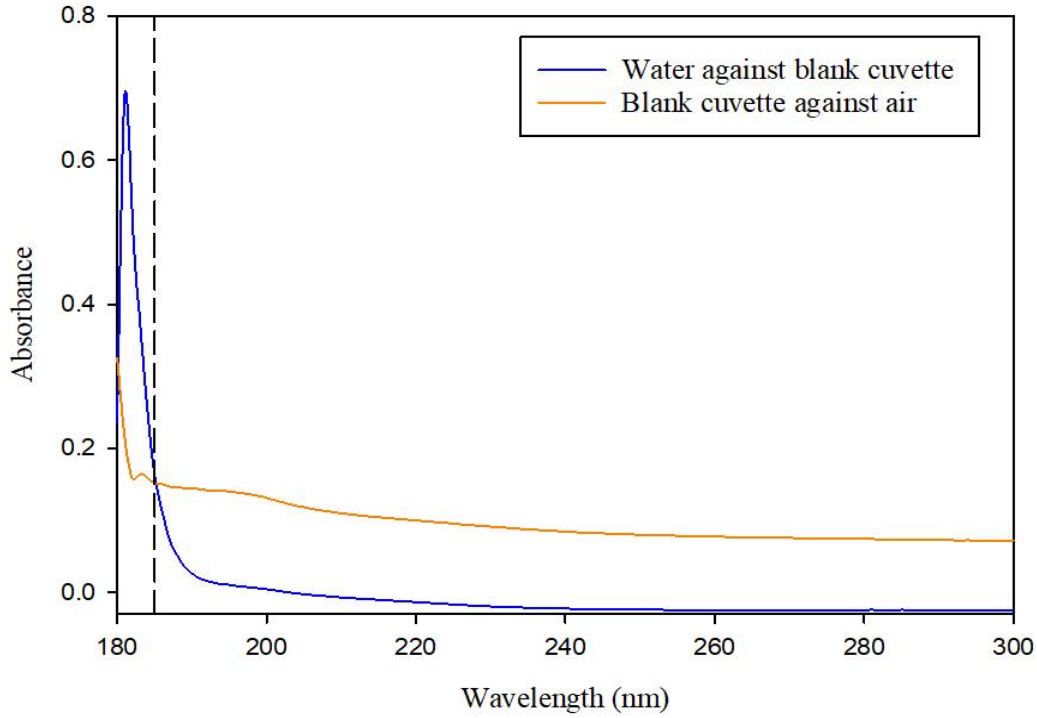

Figure 11 VUV/UVC absorption Spectra (180-300 nm): (1) blue line represents the absorbance of water subtracting absorbance of cuvette filled with nitrogen; (2) orange line is the subtract of air absorbance from absorbance of cuvette filled with nitrogen. The dashed line is a vertical line crossing the x-axis at 185 nm.

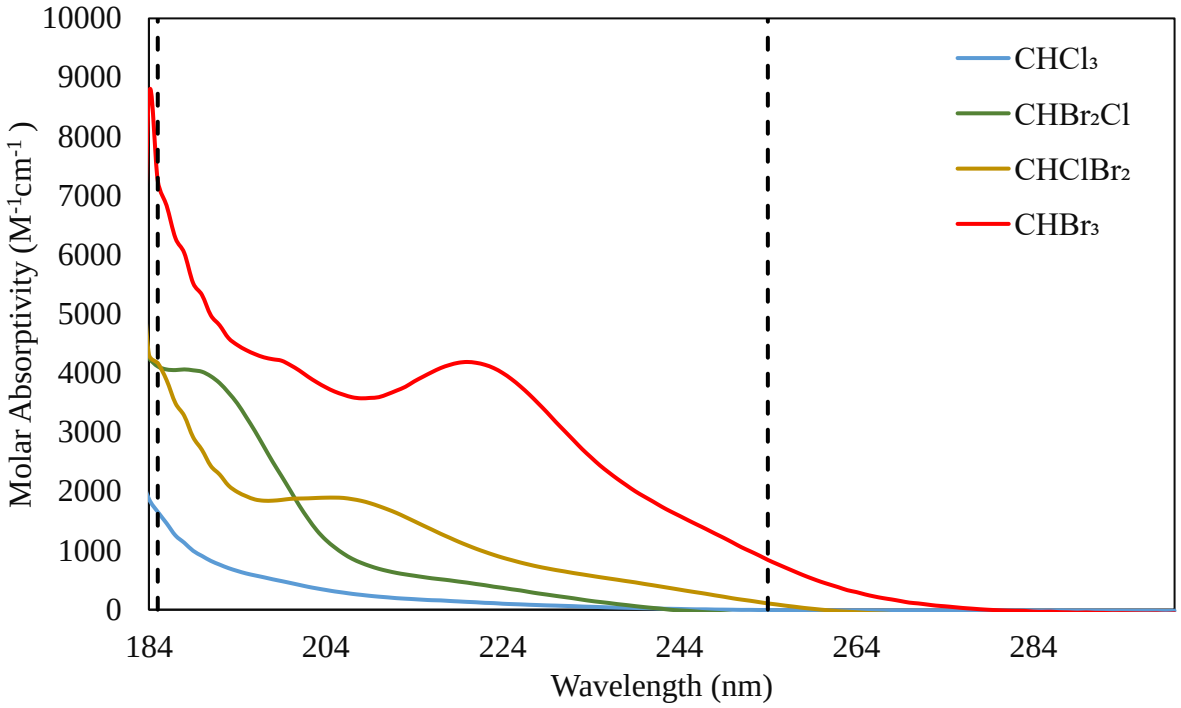

Figure 12 Molar absorption coefficient of chloroform ($CHCl_3$), dichlorobromomethane ($CHBrCl_2$), dibromochloromethane ($CHBr_2Cl$), bromoform ($CHBr_3$) ranging from 180 to 300 nm. The solvent is degassed NANO pure water. The dashed line is a vertical line crossing the x-axis at 185 nm and 254 nm.

Table 4 Molar absorption coefficient of haloforms at 185, 222, 254 nm and peak

Chemical	**Molar absorption coefficient ($M^{-1}cm^{-1}$)**			
	185 nm	222 nm	254 nm	Peak
$CHCl_3$	1655	116	0	
$CHBrCl_2$	4114	414	0	188 nm: 4064
$CHClBr_2$	4173	977	106	205 nm: 1895
$CHBr_3$	7258	4141	842	220 nm: 4189

For dual beam spectrometer, the intensity of the samples beam is defined as I; intensity of reference beam is I_0, and absorbance is presented as $\log(I_0/I)$ based on Beer-Lambert Law. To ensure the accuracy, it is better to control reading of absorbance in an ideal range (0.1-1), and the absorption of solvent and cuvette are anticipated to be small enough for detection. Figure 11 illustrates that

the absorbance of both water (blue line) and cuvette (orange line) are smaller than 0.20 at 185 nm; therefore, it is possible to measure haloform spectra by using water as solvent and cuvette with 1 mm pathlength.

Chloroform ($CHCl_3$) was observed to register measurable absorbance at a wavelength of roughly 250 nm, with a gradual increase of molar absorption coefficient at shorter wavelengths. Bromodichloromethane ($CHBrCl_2$) demonstrated a similar pattern, with measurable absorption being observed at 242 nm and had a peak absorption (4064 M^{-1} cm^{-1}) at a wavelength of 188 nm. Dibromochloromethane ($CHClBr_2$) demonstrated measurable absorption at a wavelength of 260 nm; the maximum molar absorption coefficient was 1895 M^{-1} cm^{-1} at 205 nm. Bromoform ($CHBr_3$) had a broader absorption range (180-278 nm) than other 3 THMs and one peak (4189 M^{-1} cm^{-1}) at 220 nm. At 254 nm, the molar absorption coefficient of $CHBr_3$ was 843 M^{-1} cm^{-1}, nearly eight times greater than the coefficient of $CHClBr_2$ (107 M^{-1} cm^{-1}); while $CHCl_3$ and $CHBrCl_2$ showed insignificant absorption. All four THMs absorbed radiation at 185 nm; the molar absorption coefficient of $CHCl_3$, $CHBrCl_2$, $CHBr_2Cl$, CHBr3 were 1655, 4114, 4172, 7253 M^{-1} cm^{-1}, respectively, which followed the order: $CHBr_3$ > $CHClBr_2$ > $CHBrCl_2$ > $CHCl_3$. Compounds obviously absorbed much more radiation at 185 nm than at 254 nm; compounds with greater bromine substitution absorbed UVC or VUV irradiation more strongly than their corresponding lower-brominated THMs. The C-Br bond is generally weaker than C-Cl bond; the differences in bond energy of the C-Br and C-Cl bonds are largely responsible for the differences in their absorption in the UVC range (*i.e.*, λ = 254 nm) (Hansen et al., 2013). Many other studies have confirmed that brominated compounds tend to be more susceptible to UVC photolysis than their

chlorinated analogs (Chen et al., 2010; Hansen et al., 2013). A similar trend was observed in the VUV range (185 nm).

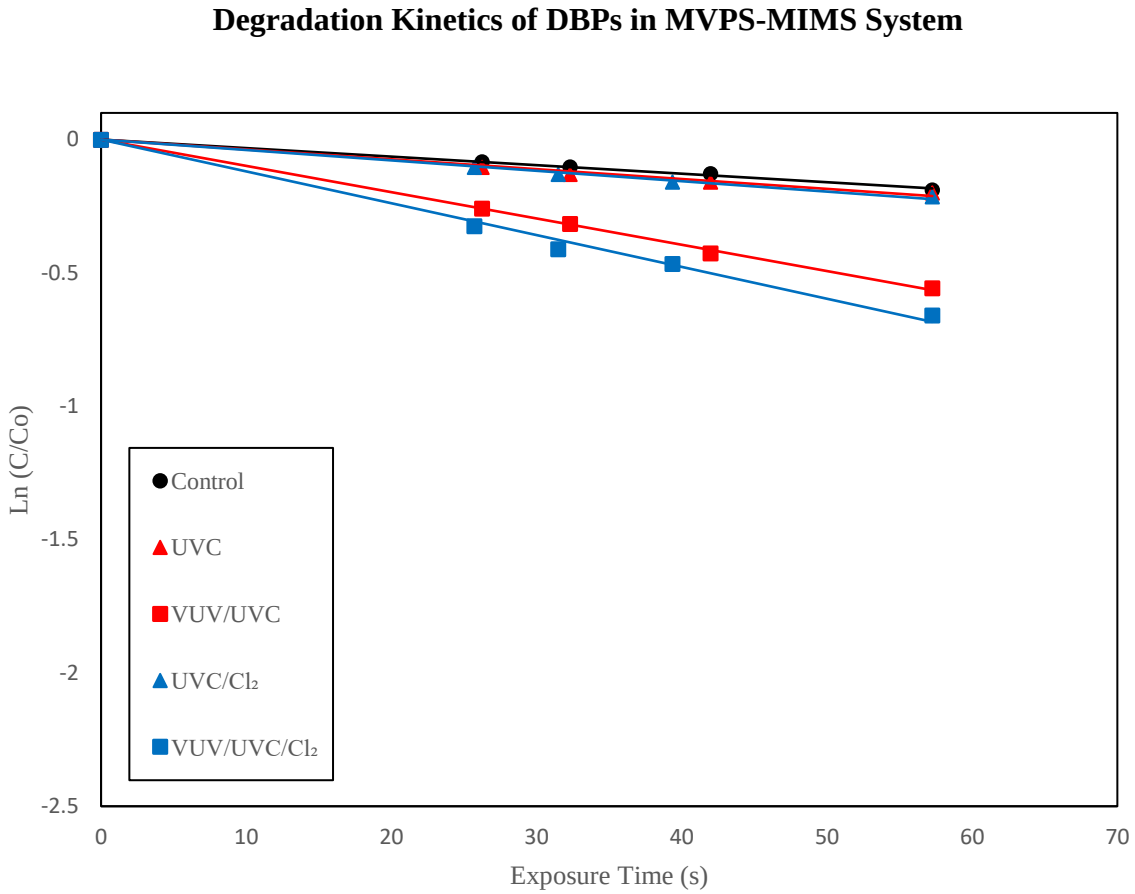

Figure 13 $CHCl_3$ Degradation

Figure 13 illustrates the degradation of $CHCl_3$ as a function of exposure time in the control as well as UVC, VUV/UVC, UVC/Cl_2 and VUV/UVC/Cl_2 processes. Regression analysis indicates that $CHCl_3$ decay followed the pseudo-first-order kinetics in those processes. The control experiment was conducted with identical experimental conditions as other irradiated experiments, but in the absence of VUV/UVC irradiation. The degradation rate is defined as the slope of regression lines. Based on comparisons in slopes of different processes, $CHCl_3$ is degraded by UVC/VUV irradiation; the descending order of loss rates is: VUV/UVC/Cl_2 > VUV/UVC > UVC/Cl_2 > UVC.

It is noted that combined VUV/UVC radiation contributed to more loss of $CHCl_3$ than UVC radiation alone. When Cl_2 was applied to irradiation process, degradation by irradiation was slightly sped up.

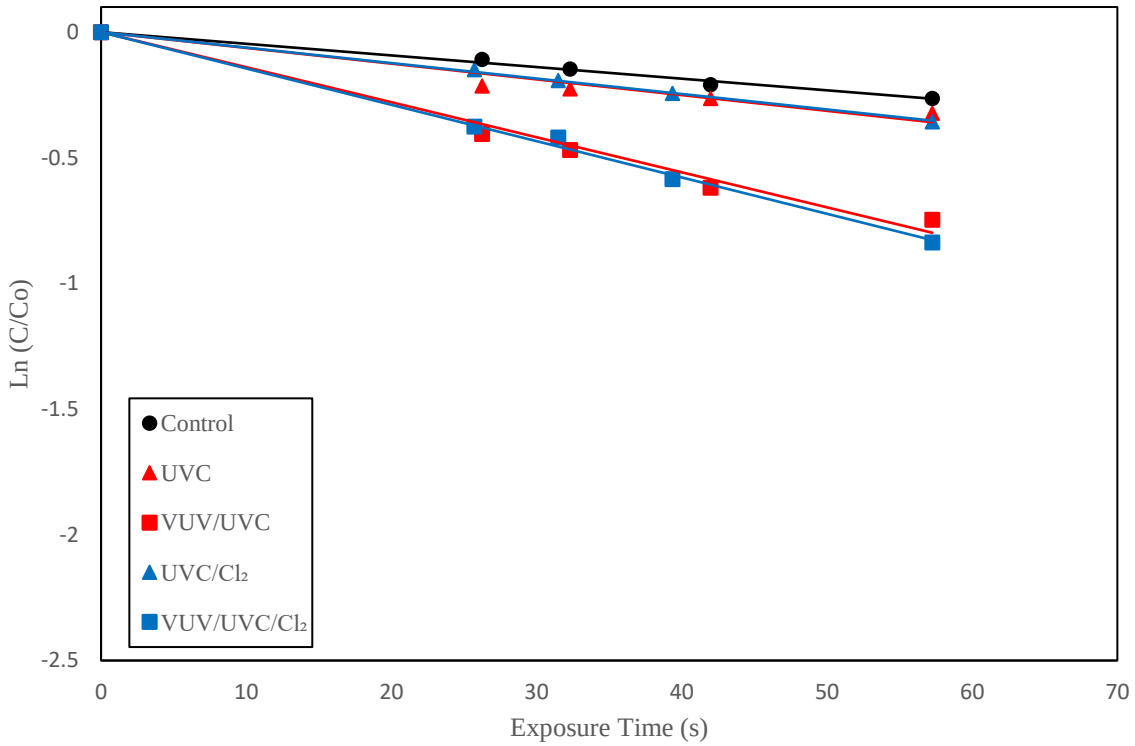

Figure 14 $CHBrCl_2$ Degradation

Figure 14 illustrates the behavior of $CHBrCl_2$ with or without UVC/VUV irradiation, in the absence or presence of Cl_2. As $CHCl_3$ performed before, $CHBrCl_2$ performs the pseudo-first-order degradation kinetics in VUV, UVC/Cl_2 and VUV/UVC/Cl_2 processes. The degradation rate of $CHBrCl_2$ in VUV/UVC process is higher than in UVC process no matter whether Cl_2 is added. The introduction of Cl_2 results in subtle changes in degradation.

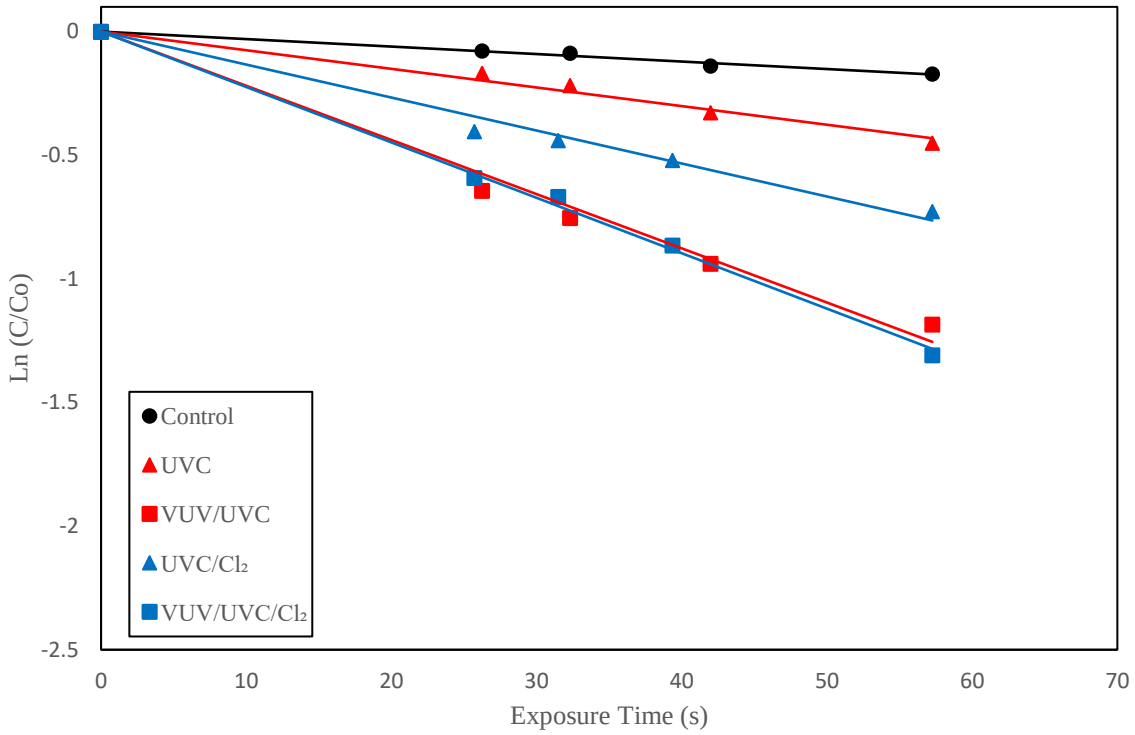

Figure 15 $CHClBr_2$ Degradation

As illustrated by Figure 15, $CHClBr_2$ is degraded by UVC/VUV irradiation, following first-order kinetics. $CHBrCl_3$ is observed to be degraded fastest in VUV/UVC/Cl_2 and slowest in UVC process; the VUV radiation induced degradation is faster than UVC radiation induced loss. The loss rates are increased when Cl_2 is applied to UVC or VUV/UVC processes.

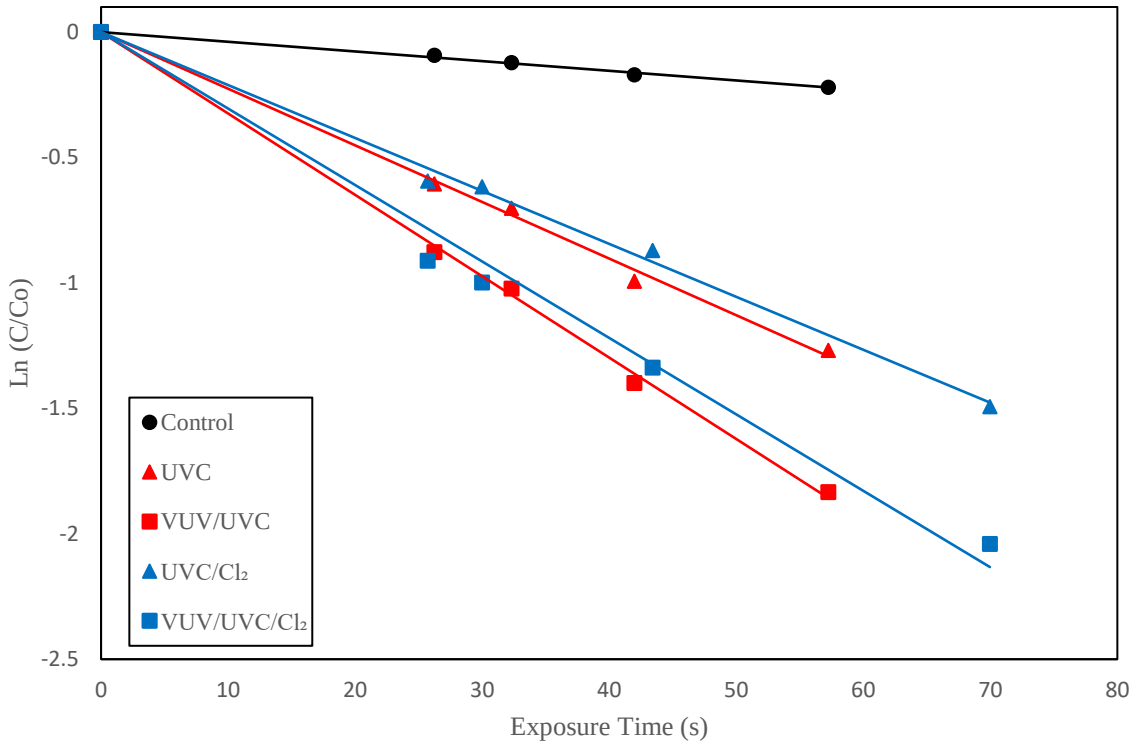

Figure 16 $CHBr_3$ Degradation

Figure 16 presents the first-order degradation kinetics of $CHBr_3$ exposed to UVC or VUV radiation and in control condition. A similar trend (like $CHCl_3$, $CHBrCl_2$ and $CHClBr_2$) was observed that VUV irradiation degraded more $CHBr_3$ than UVC irradiation. However, Cl_2 slows down the radiation induced degradation due to smaller slope (degradation rate) of UVC or VUV/UVC processes combines with Cl_2 than processes without Cl_2.

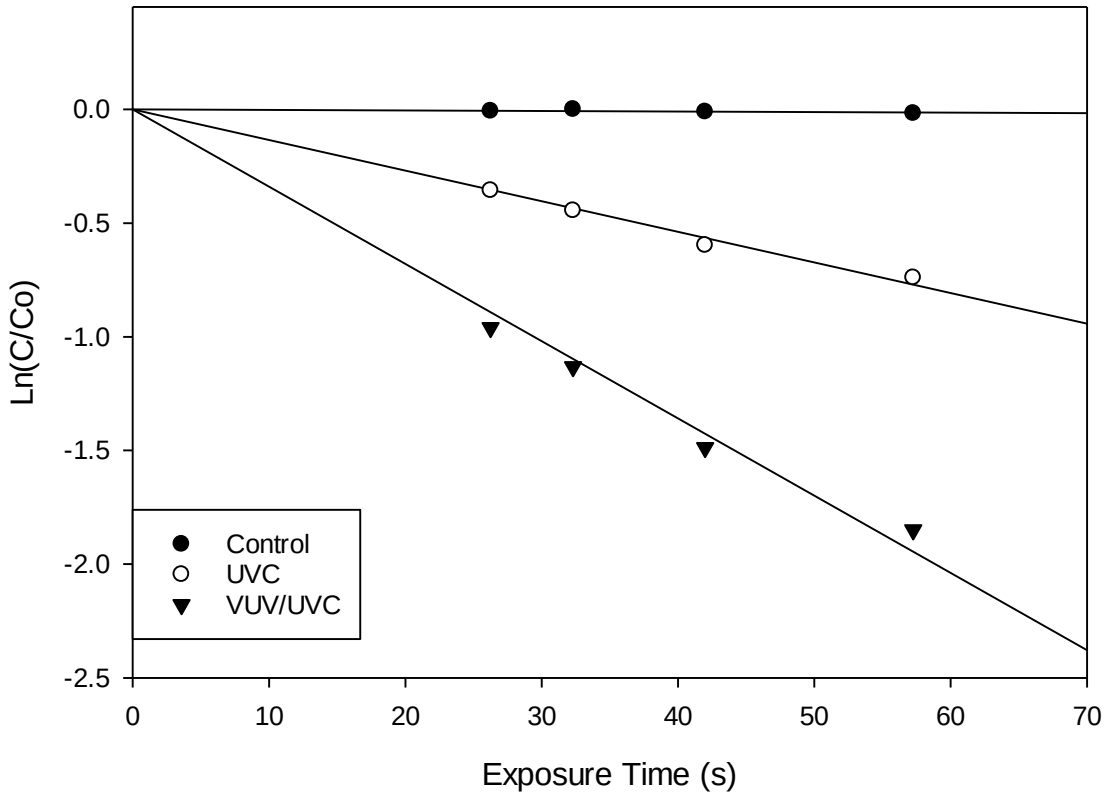

Figure 17 NH_2Cl Degradation

As shown in Figure 17, NH_2Cl is degraded more by VUV irradiation than by UVC irradiation, and degradation kinetics still follow first-order as same as THMs. The (roughly) horizontal control line illustrates that NH_2Cl is stable in the experiments.

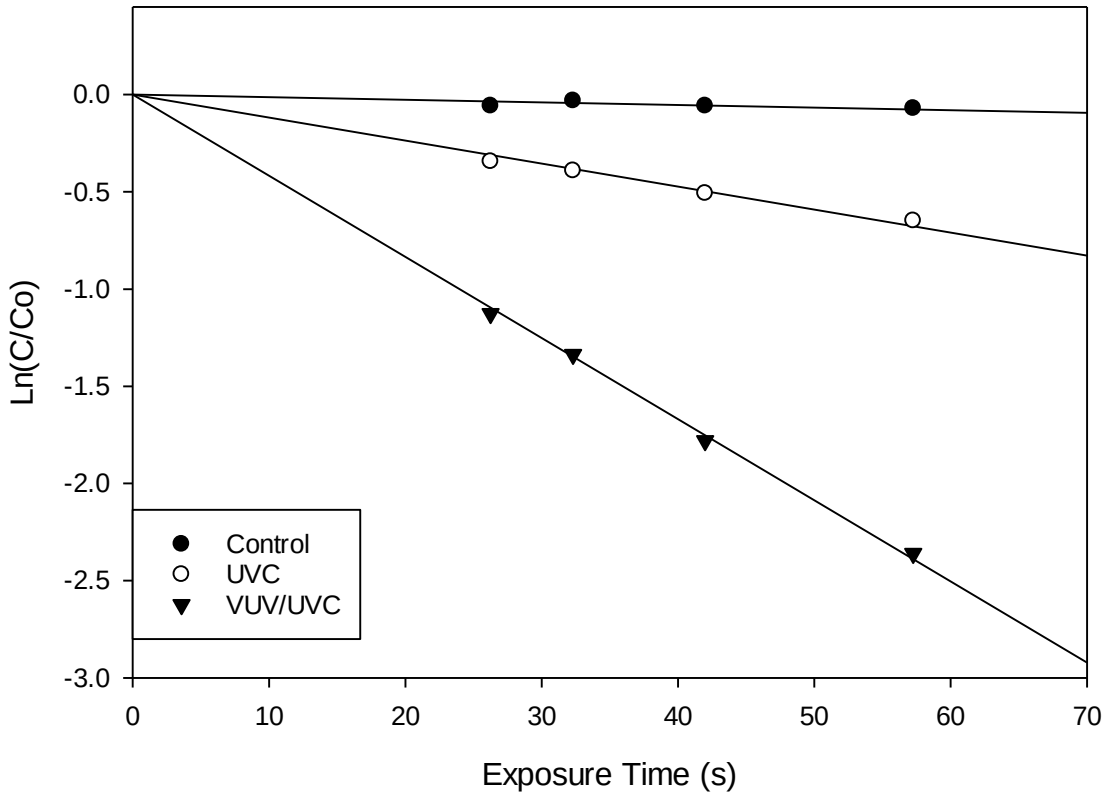

Figure 18 $NHCl_2$ Degradation

Figure 18 shows reductions in concentration of $NHCl_2$ with exposure time with or without UVC/VUV radiation. The compound follows the first-order degradation and is vulnerable to decompose in VUV range (185 nm).

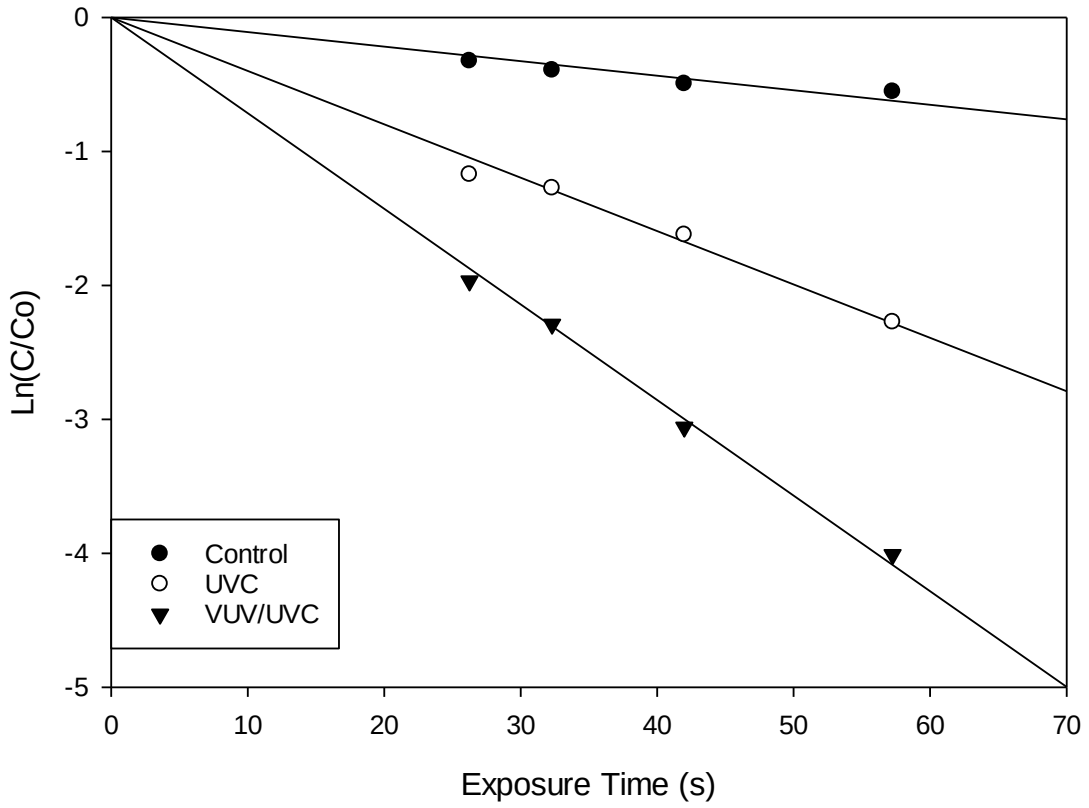

Figure 19 NCl_3 Degradation

Figure 19 illustrates the degradation of NCl_3 as a function of exposure in the absence or presence of radiation. NCl_3 was observed to be degraded with exposure time in the control experiment other than NH_2Cl and $NHCl_2$, because NCl_3 is the most volatile compound among inorganic chloramines. VUV radiation results in more loss of NCl_3 than UV radiation.

Figures 13 to 16 illustrate the degradation of THMs ($CHCl_3$, $CHBrCl_2$, $CHClBr_2$, $CHBr_3$) as a function of exposure time at pH 7 and at room temperature in the UVC, VUV/UVC, UVC/Cl_2, VUV/UVC/Cl_2 processes as well as in the control experiment. Figures 17 to 19 illustrate the degradation of inorganic chloramines (NH_2Cl, $NHCl_2$ and NCl_3) with exposure time with

controlled pH 7 and room temperature with or without UVC or VUV radiations. Regression analysis indicated that pseudo-first-order model represented the observed kinetic behavior. The control experiment was conducted in the absence of radiation.

Because these compounds are volatile, it is possible that transfer to the gas phase contributed to observed losses in the experiments. To account for the losses that may have resulted from adsorption within the MVPS and volatilization at joints between the MVPS and MIMS, a control sample was processed without UV or VUV radiations. As shown in Figures 13 to 19, decreases in concentrations with an increasing exposure time as well as a large initial reduction of the control are consistent with these loss mechanisms. The actual degradation rate (K) of each compound was estimated by subtracting the loss rate in the control experiment ($K_{control}$) from the measured rate ($K_{measured}$) in corresponding UVC, VUV/UVC, UVC/Cl_2, VUV/UVC/Cl_2 processes (equation 41). The loss rate was equal to the slope of regression lines.

$$K = K_{measured} - K_{control} \quad (41)$$

As illustrated by Figures 13 to 19, degradations of THMs and chloramines by VUV irradiation were observed to be faster than UVC irradiation, and combined VUV/UVC/Cl_2 process leaded to faster degradation of THMs except for $CHBr_3$ than the remaining processes.

Table 5 listed the degradation reaction rate constant for each DBPs, followed below equation 42 to demonstrate final results.

$$K' = K/FR \quad (42)$$

where K is the actual degradation rate constant as a function of exposure time, computed by equation 41 (s^{-1}); K' represents the degradation reaction rate constant as a function of fluence (m^2

Einstein^{-1}); FR is the UVC fluence rate (3.22×10^{-8} Einstein cm^{-2} s^{-1}) or VUV/UVC fluence rate (sum of UVC fluence rate and VUV fluence rate $=3.95\times10^{-8}$ Einstein cm^{-2} s^{-1}) according to corresponding processes. Equation 42 converts degradation rate constant based on time to rate constant based on UVC or VUV/UVC fluence by dividing fluence rates because the unit based on fluence is easier to compare with other studies using different reactors.

Table 5 Degradation reaction rate constant of DBPs based on exposure time or fluence.

DBPs	K ($\times10^{-3}$ s^{-1})				K' (m^2 Einstein^{-1})			
	UVC	VUV /UVC	UVC/Cl_2	VUV/UVC/Cl_2	UVC	VUV /UVC	UVC /Cl_2	VUV/UVC /Cl_2
$CHCl_3$	0.6	4.7	0.7	8.7	1.86	11.88	2.17	21.99
$CHBrCl_2$	1.7	9.3	1.5	9.9	5.28	23.51	4.66	25.02
$CHClBr_2$	4.5	18.9	10.3	19.4	13.97	47.77	31.97	49.03
$CHBr_3$	18.7	28.5	17.2	25.8	58.04	72.03	53.38	65.18
NH_2Cl	13.3	33.8			41.28	85.43		
$NHCl_2$	10.5	40.4			32.59	102.11		
NCl_3	29	60.5			90.00	152.92		

$CHCl_3$ demonstrated the fastest degradation (highest rate constant, 21.99 m^2 $Einstein^{-1}$) in VUV/UVC/Cl_2 process and the slowest degradation (lowest rate constant, 1.86 m^2 $Einstein^{-1}$) in UVC process. Previous researches have indicated that $CHCl_3$ does not degrade as a result of exposure to UVC radiation from low pressure Hg lamps, while exposure to radiation from medium or high pressure Hg lamps can promote $CHCl_3$ degradation (Hansen et al., 2013; Rudra, Thacker, & Pande, 2005). Consistent with previous studies, little or no $CHCl_3$ decay was observed in UVC processes without Cl_2.

Compared to $CHCl_3$, a faster degradation of $CHBrCl_2$ (high rate constant, 23.51 m^2 $Einstein^{-1}$) occurred in VUV/UVC process than in the UVC process (5.28 m^2 $Einstein^{-1}$). When Cl_2 was spiked, $CHBrCl_2$ was observed to be degraded slightly more in processes than in processes without Cl_2 introduction.

It was found that $CHClBr_2$ degraded more than $CHCl_3$ as well as $CHBrCl_2$; the reaction rate constant in UVC, VUV/UVC, UVC/Cl_2, VUV/UVC/Cl_2 processes were 13.97, 47.77. 31.97 and 49.03 m^2 $Einstein^{-1}$, respectively. The promotion effects of Cl_2 in UVC process was greater than in VUV/UVC process.

The degradation rate constants for $CHBr_3$ were 58.04 and 72.03 m^2 $Einstein^{-1}$, respectively in the UVC and VUV/UVC processes; this suggests that direct VUV photolysis and UVC photolysis of $CHBr_3$ took place at rates that were consistent with other loss mechanisms. Introduction of free chlorine resulted in slight inhibition in the rates of $CHBr_3$ decay with UVC or VUV/UVC exposure, but change was small.

The rate constant of NH_2Cl for UVC and VUV/UVC processes were 41.28 and 85.43 m^2 $Einstein^{-1}$, respectively; the latter rate constant was around 2 times greater than estimate of UVC process. $NHCl_2$ degraded more slowly than NH_2Cl was degraded in the UVC process, but an opposite trend was shown in the VUV/UVC process. The degradation rate constant of $NHCl_2$ in VUV/UVC process was roughly 3.3 times greater than the value under UVC exposure alone. NCl_3 demonstrated the fastest degradation among chloramines for both UVC and VUV exposure processes, with apparent rate constants of 90 (UVC) and 152 m^2 $Einstein^{-1}$ (VUV/UVC). Chloramines were significantly degraded by VUV/UV processes. Because of the absence of free chlorine, UV photolysis of chloramines is anticipated to be responsible for degradation. The degradation rate constant of chloramines can be ranked: $NHCl_2 < NH_2Cl < NCl_3$ consistent with the order of molar absorption coefficient has been reported at 254 nm (Ferriol & Gazet, 1988).

In general, faster degradation rates were observed for all four THMs and three chloramines in the VUV/UVC process than in the UVC according to Figures 13-19 and Table 5, presumably due to greater rates of direct photolysis by 185 nm radiation and production of hydroxyl radicals. More THMs degraded in VUV/UVC process than in UVC/Cl_2 process; in other words, VUV direct photolysis as well as oxidation by hydroxyl radicals generated from VUV photolysis of water were more beneficial than oxidation by hydroxyl radicals and chlorine radicals generated from UVC/Cl_2 process to degrade THMs. The degradation rate constant of THMs was ranked by descending in all processes: $CHBr_3 > CHClBr_2 > CHBrCl_2 > CHCl_3$, which was an agreement with the order of molar absorption coefficient described before and supported by other studies (Hansen et al., 2013). Introduction of Cl_2 (67 μM) leads to the production of hydroxyl radicals and chlorine radicals which degrade THMs. Although the presence of free chlorine altered degradation rate constants

for single THMs, little or no significant increase in THMs degradation rate was observed in VUV/UVC process in this study. It can be explained that surrounding halogens prevent carbon atoms from attacked by active radicals (Hansen et al., 2013). The future work can explore the effects of free chlorine at different concentrations.

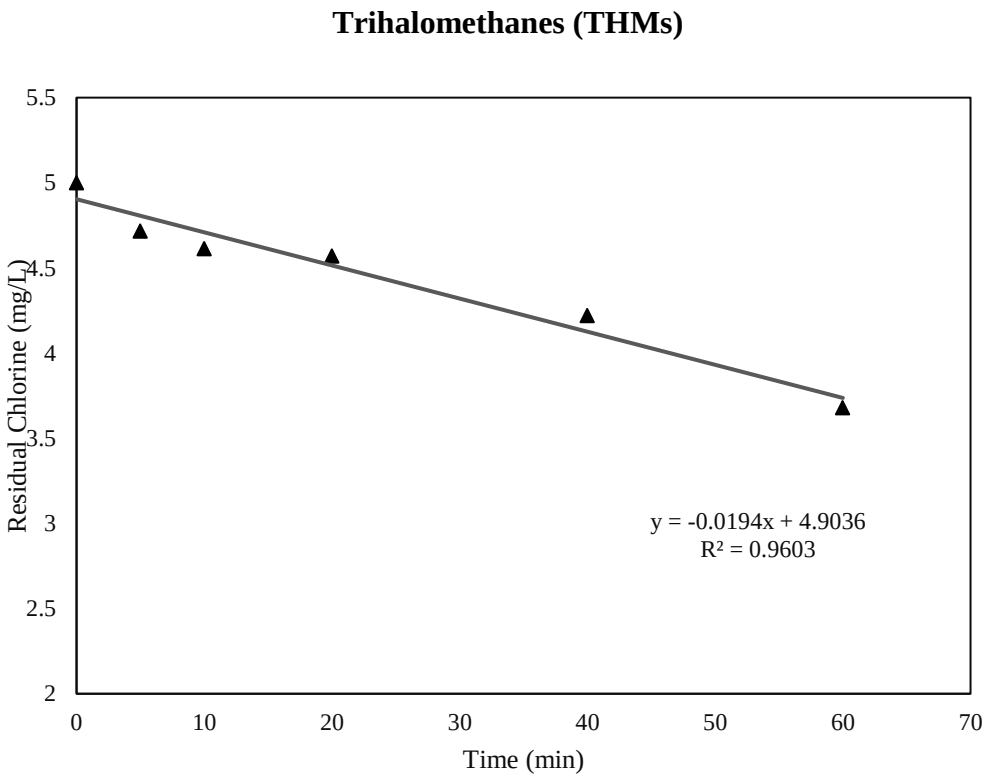

Figure 20 Residual chlorine consumption during formation of THMs

67 μM free chlorine and 6.7 μM potassium bromide were added to humic acid solution (DOC=1.45 mg/L) with controlled pH 7. The solution was stored in a 100 mL brown bottle with a stir bar which was used to mix the solution during this period. Figure 20 illustrates time-course behavior of free chlorine during this experiment. Free chlorine degraded according to a pattern that was consistent with pseudo-first-order kinetics during the THM reaction process. After 24 hours,

residual chlorine was non-detectable. Because the reactions consumed all chlorine within 24 hours, sodium bisulfite was not considered to quench excess chlorine in samples at the end of the experiment.

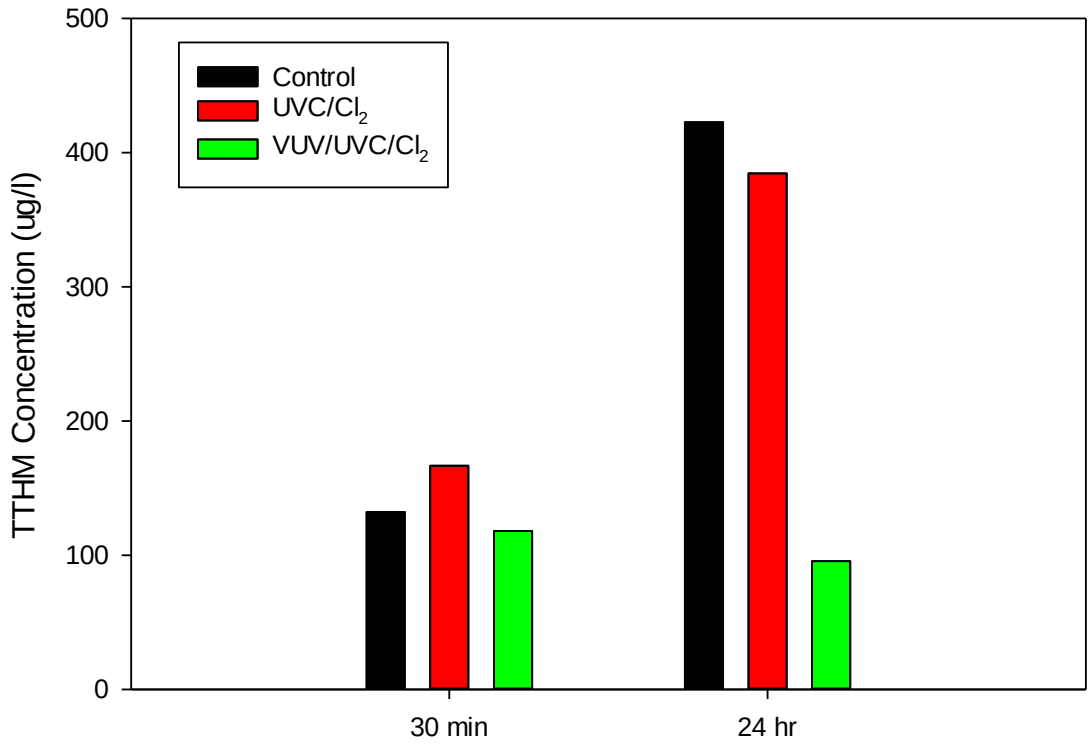

Figure 21 Concentration of formed total THMs in control, UVC/Cl_2, and VUV/UVC/Cl_2 processes at reaction times of 30 min (experiment a) and 24 hours (experiment b). The control sample received no irradiation. Initial reaction conditions: Cl_2=67 µM; Br^-=6.7 µM; DOC=1.45 mg/L; pH =7; T=23 °C.

In the control experiment, the concentration of total THMs increased from 132 to 422 µg/L, an increase of a factor of roughly 3.2 times over the 24-hr reaction period. Interestingly, an initial increase in total THM concentration was observed in the presence of UVC radiation. It is possible that UVC radiation altered the structures of NOM molecules into compounds with more hydrophobic fraction that reacted more favorable with free chlorine or free bromine to produce

THMs (Buchanan et al., 2006). Wang et al (2017) indicated that large molecular weight substances were degraded as 4.5 times faster than medium molecular weight substances, thus NOM molecules were vulnerable to attack by radiation during initial period. In the presence of UVC radiation, the concentration of total THMs increased from 166 to 384 μg/L, but of the relative and absolute increases of TTHM were smaller than in the control. The difference between total THM concentration of control and UVC process at a reaction time of 24 hours might result from a removal of THM precursors like NOM and by UVC irradiation, or from photolysis of free chlorine.

In the VUV/UVC/Cl_2 process, total THM concentration decreased from 118 to 96 μg/L over the 24-hr reaction period, which suggested smaller formation rate than degradation rate. A large difference between total THM concentration of VUV/UVC/Cl_2 experiment and UVC/Cl_2 experiment may involve in VUV or UVC direct photolysis of THMs, oxidation by reactive radicals (·OH, H·, Cl· and a number of intermediate radicals) or NOM degradation. VUV/UVC radiation has been reported to degrade more NOM and to generates more hydroxyl radicals than UVC radiation; NOM is assumed to be degraded by UVC irradiation and furthermore the remaining NOM is mineralized by oxidizing agents (Imoberdorf & Mohseni, 2011). Also, the aforementioned degradation kinetics analysis for individual THMs stated that VUV/UVC process was a more efficient AOP than either UVC or UVC/Cl_2 process.

For purposes of this experiment, trihalomethane formation potential (THMFP) was defined as the concentration of total THMs after 24 hr. Based on this definition, THMFP was 422, 384 and 95 μg/L in the control, UVC/Cl_2 and VUV/UVC/Cl_2 processes, respectively. UVC/Cl_2 resulted in a 9% reduction of THMFP, whereas 77% of THMFP was degraded by VUV/UVC/Cl_2. Lamsal et

al., (2011) has demonstrated the reduction of 15 % for THMFP in UV alone, the reduction of 77 % for THMFP in H_2O_2/UV as well as the reduction of 75 % for THMFP in O_3/UV at a fluence of 1140 mJ cm^{-2}. Compared to other AOPs, VUV/UVC/Cl_2 process showed similar effects on THMFP (77 % reduction) with H_2O_2/UV process, greater than the remaining processes.

Effects of free chlorine

UVC radiation is not able to photolyze water but induces degradation of free chlorine to produce hydroxyl radicals and other intermediates (equations 5 to 8). Hence, UVC/Cl_2 was anticipated to degrade more organic matters than UVC, which has been supported in Wang et al., (2017). The reduction in concentration of DOC was reported to be raised to 15.1-18.6% by synergistic effects of UVC/Cl_2 (Wang et al., 2017).

In VUV/UVC process, photolysis of free chlorine generates hydroxyl radicals to slightly degrade more $CHCl_3$, $CHBrCl_2$ and $CHClBr_2$. At the same time, the depletion of Cl_2, accompanying with the formation of secondary radical (·OCl) as well as the consumption of hydroxyl radicals, is greater in VUV/UVC/Cl_2 process than in UVC processes (equations 14 and 15). The THM formation may be inhibited due to a lack of available free chlorine.

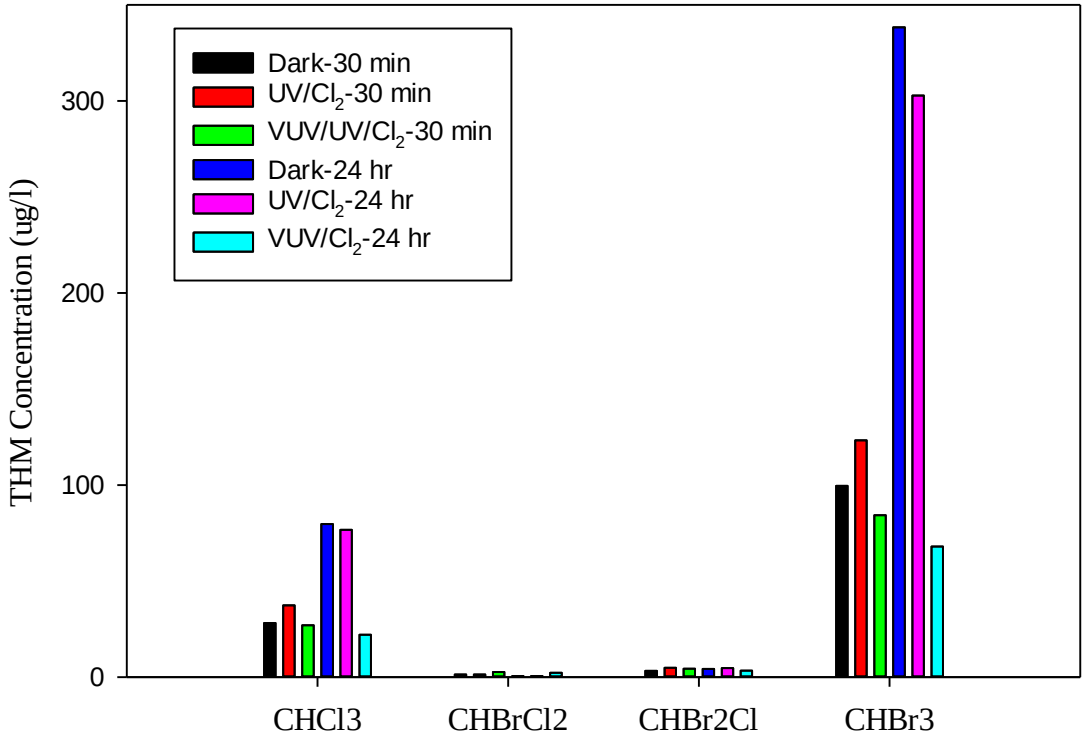

Figure 22 Formation of THM species in the control, UVC/Cl_2 and VUV/UVC/Cl_2 experiments. Concentration was measured at 30 min in experiment (a) and at 24 hours in experiment (b).

Table 6 Formation of THM species after 30 min as well as after 24 hours in (dark) control, UVC/Cl_2 and VUV/UVC/Cl_2 experiments (experiment a & b)

Compound	Concentration @ 30 min (µg/L)			Concentration @ 24 hours (µg/L)		
	Control	UVC/Cl_2	VUV/UVC/Cl_2	Control	UVC/Cl_2	VUV/UVC/Cl_2
$CHCl_3$	28.2	37.4	27.0	79.7	76.6	22.1
$CHBrCl_2$	1.40	1.40	2.64	0.57	0.52	2.27
$CHBr_2Cl$	3.24	4.80	4.34	4.28	4.65	3.37
$CHBr_3$	99.5	1.23×10^2	84.2	3.38×10^2	3.02×10^2	68.0
Total THMs	1.32×10^2	1.66×10^2	1.18×10^2	4.22×10^2	3.84×10^2	95.7

As illustrated by Figure 22, $CHBr_3$ was the predominant THM compound, both in terms of total THMs and among the brominated compounds, because of a small Cl_2: Br^- ratio (10 μM Cl_2 /μM Br^-). Compared to $CHBr_3$ and $CHCl_3$, $CHBrCl_2$ and $CHClBr_2$ were present at substantially lower concentration and exhibited to insignificant to the formation of total THMs. The conditions of reaction for this experiment were favorable to formation of the fully-brominated and fully-chlorinated THMs. Other reaction conditions will likely yield different distributions among these compounds.

Initially, brominated THMs demonstrated more increase or reduction in concentrations than chlorinated THMs in corresponding UVC/Cl_2 or VUV/UVC/Cl_2 process respectively, which could be explained by higher molar absorption coefficient and degradation rate constant of brominated THMs than chlorinated THMs. After 24 hours, both $CHCl_3$ and $CHBr_3$ demonstrated substantial degradation as a result of the VUV/UVC/Cl_2 process, while $CHBr_2Cl$ decreased slightly and $CHBrCl_2$ increased.

In term of individual compounds of THMs, decreases in $CHCl_3$ and $CHBr_3$ formation potential were higher by VUV/UVC/Cl_2 than by UVC/Cl_2. For example, 3.89 % (3.1 μg/L) and 72.31% (57.6 μg/L) of $CHCl_3$ were removed by UVC/Cl_2 and VUV/UVC/Cl_2 processes, respectively, while the removal percentage of $CHBr_3$ reached up to 10.49% (36 μg/L) and 79.91% (270 μg/L) from the UVC/Cl_2 and VUV/UVC/Cl_2 treatment processes, respectively. The removal efficiency by VUV/UVC/Cl_2 was greater than by UV/H_2O_2 reported in Rudra et al., (2015). Because the UVC fluence in both treatments were roughly identical, VUV radiation contributed to high removal of $CHCl_3$ and $CHBr_3$ in VUV/UVC/Cl_2 process, consistent with degradation analysis of

individual component of THMs. The removal efficiency was nearly raised by 24 times for $CHCl_3$ and around 8 times for $CHBr_3$.

Although UV fluence for disinfection ranged from 40 to 100 mJ cm^{-2}, previous work classified UV radiation in the order of 1000 mJ cm^{-2} as low AOP fluence and subjected the UV range of 3000-5000 mJ cm^{-2} to high fluence (Wang et al., 2015). The pumping flow rate for THM experiment is 3 mL/min and hence irradiation time is equal to tube volume divided by flow rate (t=42 s). UVC and VUV/UVC fluence were estimated to be 713 and 917 mJ cm^{-2} through multiplying VUV/UVC fluence rate by irradiation time (42 s), and both of these estimates were in the low AOP fluence range. In contrast to the AOP/post-chlorination experiments investigated in Wang et al., (2015), low AOP fluence may lead to reductions in formation potential of either total THM or individual components by pre-chlorination/AOP process.

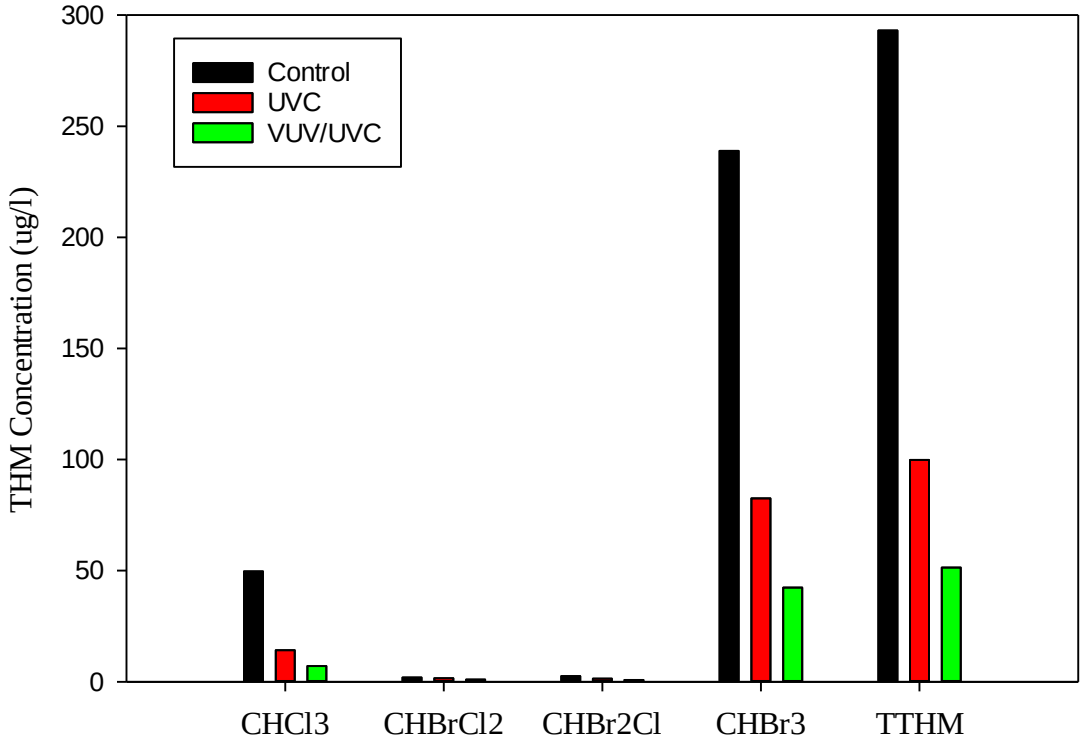

Figure 23 Degradation of THMs by control, UVC, VUV/UVC processes in experiment (c). Irradiation experiment follows by 24-hrs formation of THM in the dark. No residual chlorine. The control sample receives no radiation. Initial reaction conditions: Cl_2=67 μM; Br^-=6.7 μM; DOC=1.45 mg/L; pH =7; T=23 °C.

Figure 23 illustrates the degradation of individual THMs and total THMs that reacted over a 24-hrs period with or without exposure to UV radiation (either UVC or VUV/UVC). In contrast to previous experiments, samples were incubated for 24 hours in the dark at first and then subjected to UVC or VUV/UVC radiation prior to measurement of THM concentrations. There is no residual chlorine left in the solution.

The main goal of this experiment is to examine effects of UVC or VUV/UVC radiation on removal of mixed THMs species. Consistent with previous experiments, $CHBr_3$ and $CHCl_3$ were still the

major species among total THMs. Significant reductions in total THMFP and individual THM species formation potential were observed in both UVC and VUV/UVC processes. The removal efficiencies of the respective THMs ($CHCl_3$, $CHBrCl_2$, $CHClBr_2$, $CHBr_3$) were 71.43%, 15.32%, 41.94%, 65.46 % in the UVC process and 85.71%, 46.85%, 66.91% as well as 82.26 % in VUV/UVC process. Through comparisons between these removal efficiencies, VUV/UVC provided greater degradation of THMs than UVC alone. Total THM concentration in control experiment was 294 μg/L which exceeded the EPA limit of 80 μg/L. The reduction of total THMs was 66 % (195 μg/L) in UVC process, while promotion effects of VUV/UVC treatment demonstrated degradation of 82 %, (243 μg/L) with a final TTHM concentration of 51 μg/L.

Table 7 Removal efficiency of THMs in mixed culture (measured in experiment (c)) and in individual condition (Degradation kinetics of pure DBPs experiment)

Compound	**UVC (Mix)**	**UVC (individual)**	**VUV/UVC (Mix)**	**VUV/UVC (individual)**
$CHCl_3$	71.43%	2.49%	85.71%	17.91%
$CHBrCl_2$	15.32%	6.89%	46.85%	32.33%
$CHBr_2Cl$	41.94%	17.22%	66.91%	54.79%
$CHBr_3$	65.46%	54.40%	82.26%	69.79%
TTHM	65.95%		82.48%	

Table 7 demonstrates the removal efficiency observed in culture with mixed THM species and individual THMs experiment. The removal efficiency by UVC or VUV irradiation in mixed culture was found to be higher than removal efficiency of individual THMs. There is no powerful evidence to explain this observation, it need more exploration in the future.

CONCLUSIONS

The major purpose of this project was to investigate the effects of VUV/UVC irradiation on the behaviors of THMs and inorganic chloramines. Chloroform is known to be essentially non-responsive to UVC radiation alone; THM responses to UVC radiation increase with the degree of bromination. However, the inclusion of vacuum UV radiation (185 nm) allows for improvement in the rate of direct photolysis and for formation of reactive intermediates (*e.g.*, HO·) that can also cause degradation.

To determine the absorption of THMs in the vacuum UV range (*e.g.*, 185 nm), it is important to account for absorbance by non-target constituents of the system, including water, the cuvette, and dissolved gases. A descending order of molar absorptivity at 185 and 254 nm was ranked: $CHBr_3$ > $CHClBr_2$ > $CHBrCl_2$ > $CHCl_3$. At both wavelengths, the degree of bromine substitution strongly influenced absorption behavior.

The degradation rate of THMs for UVC or VUV/UVC radiation followed a similar pattern, with the rate generally increasing with the degree of bromination. The degradation behavior of these compounds followed a pattern that was consistent with (pseudo-)first-order kinetics. Chloramines were also found to follow first order degradation and generally demonstrated more rapid decay than the THMs.

These experiments also demonstrated some of the capabilities of a system that integrated a mini-fluidic VUV/UVC photoreaction system with membrane introduction mass spectrometry (MVPS-MIMS) for quantification of the responses of volatile compounds to UVC or VUV/UVC exposure.

Previous research has typically involved UV exposure and sample analysis as separate processes, often involving GC-MS or HPLC. By directly coupling with MIMS, reaction progress could be monitored in real time. However, losses were observed in the system, probably caused by volatilization and adsorption, thus control experiments were required to account for these sources of error.

The MVPS used in this research allows exposure to UVC radiation (254 nm) or VUV/UVC radiation (185/254nm). The effects of combined VUV/UVC radiation greater than the sum of UVC plus VUV, suggesting that synergism between these exposure processes may have occurred.

Based on the observed rates of degradation for the THMs and chloramines, VUV/UVC irradiation promoted faster degradation than UVC alone. When chlorine was added to the reaction mixture, all three THMs except bromoform degraded more rapidly than with their corresponding processes without chlorine. When individual effects and combined effects were compared, the combined VUV/UVC/Cl_2 process was 2-5 times better than the individual processes.

An experiment was conducted to examine the effects of VUV/UVC/Cl_2 on solutions that contained a mixture of THMs. The molar ratio of bromide to free chlorine was higher in this experiment than will exist in most water treatment applications, resulting in preferential $CHBr_3$ formation (Buchanan et al., 2006; Chang et al., 1996; Guo et al., 2016; Symons et al., 1993). For this condition, the VUV/UVC irradiation process was more efficient than the UVC process for degradation of THMs. Also, VUV/UVC/Cl_2 was observed to reduce more THMFP than conventional UVC/Cl_2 and remove abundant THM precursors. Combined with the results from degradation kinetics analysis, VUV/UVC/Cl_2 was the best option to remove THMs.

The research only investigated the potential application of VUV on drinking water treatment in the lab scale. Future research could focus on the following: (1) investigate removal efficiency of other DBPs like HAAs in VUV/UVC/Cl_2 processes. (2) investigate the degradation kinetics of other DBPs once exposed to VUV radiation. (3) Compare the performance of UVC/Cl_2 and VUV/UVC/Cl_2 on tap water.

LIST OF REFERENCE

APHA, AWWA, & WEF. (1998). *Standard methods for the examination of water and wastewater*. American Public Health Association.

Bond, T., Goslan, E. H., Parsons, S. A., & Jefferson, B. (2012). A critical review of trihalomethane and haloacetic acid formation from natural organic matter surrogates. *Environmental Technology Reviews*, *1*(1), 93–113. https://doi.org/10.1080/09593330.2012.705895

Boorman, G. A., Dellarco, V., Dunnick, J. K., Chapin, R. E., Hunter, S., Hauchman, F., … Sills, R. C. (1999). Drinking water Disinfection Byproducts: Review and Approach to toxicity evaluation.

Boos, R. N. (1948). Quantitative Colorimetric Microdetermination of Methanol with Chromotropic Acid Reagent. *Analytical Chemistry*, *20*(10), 964–965. https://doi.org/10.1021/ac60022a032

Buchanan, W., Roddick, F., & Porter, N. (2006). Formation of hazardous by-products resulting from the irradiation of natural organic matter: Comparison between UV and VUV irradiation. *Chemosphere*, *63*(7), 1130–1141. https://doi.org/10.1016/j.chemosphere.2005.09.040

Buchanan, W., Roddick, F., & Porter, N. (2008). Removal of VUV pre-treated natural organic matter by biologically activated carbon columns. *Water Research*, *42*(13), 3335–3342. https://doi.org/10.1016/J.WATRES.2008.04.014

Buenker, R. J., Olbrich, G., Schuchmann, H. P., Schumann, B. L., & von Sonntag, C. (1984). Photolysis of Methanol at 185 nm. Quantum Mechanical Calculations and Product Study. *Journal of the American Chemical Society*, *106*(16), 4362–4368. https://doi.org/10.1021/ja00328a011

Champagne, P. (2008). An investigation on parameters for modeling THMs formation, (March).

Chang, E. E., Chao, S., Chiang, P., Lee, J., Chao, S.-H., Chiang, P.-C., & Lee, J.-F. (1996). Toxicological & Environmental Chemistry Effects of chlorination on THMs formation in raw water EFFECTS OF CHLORINATION ON THMs FORMATION IN RAW WATER. *Toxicological & Environmental Chemistry Toxicological and Environmental Chemistry*, *56*(56), 1–4. https://doi.org/10.1080/02772249609358364

Chen, B., Lee, W., Westerhoff, P. K., Krasner, S. W., & Herckes, P. (2010). Solar photolysis kinetics of disinfection byproducts. *Water Research*, *44*(11), 3401–3409. https://doi.org/10.1016/J.WATRES.2010.03.014

Department of Health Vermont. (2012). Public Health Review of Monochloramine. Retrieved from http://www.healthvermont.gov/sites/default/files/documents/2016/12/Env_DW_public_health_review_of_monochloramine.pdf

EPA. (n.d.). Chloramines in Drinking Water. Retrieved from https://www.epa.gov/dwreginfo/chloramines-drinking-water

EPA. (1992). Monochloramine (CASRN 10599-90-3) | IRIS | US EPA. Retrieved from https://cfpub.epa.gov/ncea/iris/iris_documents/documents/subst/0644_summary.pdf

EPA. (1994). Drinking Water criteria document for chloramines. Retrieved from https://www.epa.gov/sites/production/files/2015-09/documents/dwchloramine.pdf

Ferriol, M., & Gazet, J. (1988). Ultraviolet absorption spectra of chloramines and chlorine in carbon tetrachloride. *Analytica Chimica Acta*, *209*, 321–325. https://doi.org/10.1016/S0003-2670(00)84580-8

Gonzalez, M. G., Oliveros, E., Wörner, M., & Braun, A. M. (2004). Vacuum-ultraviolet photolysis of aqueous reaction systems. *Journal of Photochemistry and Photobiology C: Photochemistry Reviews*, *5*(3), 225–246. https://doi.org/10.1016/j.jphotochemrev.2004.10.002

Guo, Z. B., Lin, Y. L., Xu, B., Hu, C. Y., Huang, H., Zhang, T. Y., … Gao, N. Y. (2016). Factors affecting THM, HAN and HNM formation during UV-chlor(am)ination of drinking water. *Chemical Engineering Journal*, *306*, 1180–1188. https://doi.org/10.1016/j.cej.2016.08.051

Hansen, K. M. S., Zortea, R., Piketty, A., Vega, S. R., & Andersen, H. R. (2013). Photolytic removal of DBPs by medium pressure UV in swimming pool water. *Science of the Total Environment*, *443*, 850–856. https://doi.org/10.1016/j.scitotenv.2012.11.064

Heit, G., Neuner, A., Saugy, P. Y., & Braun, A. M. (1998). Vacuum-UV (172 nm) actinometry. The quantum yield of the photolysis of water. *Journal of Physical Chemistry A*, *102*(28), 5551–5561. https://doi.org/10.1021/jp980130i

Horwitz, W., & Latimer, G. W. (2005). *Official methods of analysis of AOAC International* (18th ed.). Gaithersburg Md.: AOAC International. Retrieved from http://www.worldcat.org/title/official-methods-of-analysis-of-aoac-international/oclc/62751475

Hua, G., & Reckhow, D. A. (2012). Evaluation of bromine substitution factors of DBPs during chlorination and chloramination. *Water Research*, *46*(13), 4208–4216. https://doi.org/10.1016/j.watres.2012.05.031

Imoberdorf, G., & Mohseni, M. (2011). Degradation of natural organic matter in surface water using vacuum-UV irradiation. *Journal of Hazardous Materials*, *186*(1), 240–246. https://doi.org/10.1016/j.jhazmat.2010.10.118

Ivannenko, T., & Zogorski, J. S. (2006). Sources and Occurrence of Chloroform and Other Trihalomethanes in Drinking-Water Supply Wells in the United States , 1986 – 2001. *U.S. Geological Survey Scientific Investigations Report 2006-5015*, 13.

J.J., R. (1974, January 1). FORMATION OF HALOFORMS DURING CHLORINATION OF NATURAL WATERS. JOURNAL OF WATER TREATMENT EXAMINATION. Retrieved from http://www.sid.ir/En/Journal/ViewPaper.aspx?ID=61871

Jacobs, J. H., Spaan, S., van Rooy, G. B. G. J., Meliefste, C., Zaat, V. A. C., Rooyackers, J. M., & Heederik, D. (2007). Exposure to trichloramine and respiratory symptoms in indoor swimming pool workers. *The European Respiratory Journal*, *29*(4), 690–8. https://doi.org/10.1183/09031936.00024706

Jafvert, C. T., & Valentine, R. L. (1992). Reaction scheme for the chlorination of ammoniacal water. *Environmental Science & Technology*, *26*(3), 577–586. https://doi.org/10.1021/es00027a022

Jin, J., El-Din, M. G., & Bolton, J. R. (2011). Assessment of the UV/Chlorine process as an advanced oxidation process. *Water Research*, *45*(4), 1890–1896. https://doi.org/10.1016/J.WATRES.2010.12.008

Jin, S., Mofidi, A. a, Asce, M., & Linden, K. G. (2007). Actinometry , Biodosimetry , and Mathematical Techniques. *Journal of Environmental Engineering*, *132*(8), 831–842.

Judd, S. J., & Jeffrey, J. A. (1995). Trihalomethane formation during swimming pool water disinfection using hypobromous and hypochlorous acids. *Water Research*, *29*(4), 1203–1206. https://doi.org/10.1016/0043-1354(94)00230-5

Krasner, S. W., McGuire, M. J., Jacangelo, J. G., Patania, N. L., Reagan, K. M., & Aieta, E. M. (1989). The Occurrence of Disinfection By-products in US Drinking Water (PDF). *Journal - American Water Works Association*, *81*(8), 41–53. https://doi.org/10.2307/41292789

Krasner, S. W., Westerhoff, P., Chen, B., Rittmann, B. E., & Amy, G. (2009). Occurrence of Disinfection Byproducts in United States Wastewater Treatment Plant Effluents. *Environmental Science & Technology*, *43*(21), 8320–8325. https://doi.org/10.1021/es901611m

Kumar, S., Forand, S., Babcock, G., & Hwang, S. A. (2014). Total trihalomethanes in public drinking water supply and birth outcomes: A cross-sectional study. *Maternal and Child Health Journal*, *18*(4), 996–1006. https://doi.org/10.1007/s10995-013-1328-4

Lamsal, R., Walsh, M. E., & Gagnon, G. A. (2011). Comparison of advanced oxidation processes for the removal of natural organic matter. *Water Research*, *45*(10), 3263–3269. https://doi.org/10.1016/J.WATRES.2011.03.038

Li, M., Qiang, Z., Hou, P., Bolton, J. R., Qu, J., Li, P., & Wang, C. (2016). VUV/UV/Chlorine as an Enhanced Advanced Oxidation Process for Organic Pollutant Removal from Water: Assessment with a Novel Mini-Fluidic VUV/UV Photoreaction System (MVPS). *Environmental Science and Technology*, *50*(11), 5849–5856. https://doi.org/10.1021/acs.est.6b00133

Masschelein, W., & Rice, R. (2002). *Ultraviolet Light in Water and Wastewater Sanitation*. CRC Press. https://doi.org/10.1201/9781420032178

NIOSH. (1994). Formaldehyde: Method 3500. *Manual of Analitical Methods*, (2), 3–5.

Oppenländer, T., & Schwarzwälder, R. (2002). Vacuum-UV Oxidation (H2O-VUV) with a Xenon Excimer Flow-Trough Lamp at 172 nm: Use of Methanol as Actinometer for VUV Intensity Measurement and as Reference Compound for OH-Radical Competition Kinetics in Aqueous Systems. *Journal of Advanced Oxidation Technologies*, *5*(2), 155–163. Retrieved from http://www.ingentaconnect.com/content/stn/jaots/2002/00000005/00000002/art00006

PANYAKAPO, M., SOONTORNCHAI, S., & PAOPUREE, P. (2008). Cancer risk assessment from exposure to trihalomethanes in tap water and swimming pool water. *Journal of Environmental Sciences*, *20*(3), 372–378. https://doi.org/10.1016/S1001-0742(08)60058-3

Peng, D., Saravia, F., Abbt-Braun, G., & Horn, H. (2016). Occurrence and simulation of trihalomethanes in swimming pool water: A simple prediction method based on DOC and mass balance. *Water Research*, *88*, 634–642. https://doi.org/10.1016/j.watres.2015.10.061

Resolution Oeno. (2009). Method OIV-MA-AS323-01B Type IV method, 2–5.

Richardson, S. D. (2003). Disinfection by-products and other emerging contaminants in drinking water. *TrAC Trends in Analytical Chemistry*, *22*(10), 666–684. https://doi.org/10.1016/S0165-9936(03)01003-3

Rudra, A., Thacker, N. P., & Pande, S. P. (2005). HYDROGEN PEROXIDE AND ULTRAVIOLET IRRADIATIONS IN WATER TREATMENT. *Environmental Monitoring and Assessment*, *109*, 189–197. https://doi.org/10.1007/s10661-005-6372-0

Sakai, H., Tokuhara, S., Murakami, M., Kosaka, K., Oguma, K., & Takizawa, S. (2016). Comparison of chlorination and chloramination in carbonaceous and nitrogenous disinfection byproduct formation potentials with prolonged contact time. *Water Research*, *88*, 661–670. https://doi.org/10.1016/j.watres.2015.11.002

Scholes, M. L., SCHUCHMANNt, M. N., & Von Sonntag, C. (1992). International Journal of Radiation Biology Enhancement of Radiation-induced Base Release from Nucleosides in Alkaline Solution: Essential Role of the O Sonntag (1992) Enhancement of Radiation-induced Base Release from Nucleosides in Alkaline Solution: Ess. *International Journal of Radiation Biology INT . J. RADIAT . BIOL*, *614*(4), 443–449. https://doi.org/10.1080/09553009214551191

Shang, C., & Blatchley, E. R. (1999). Differentiation and quantification of free chlorine and inorganic chloramines in aqueous solution by MIMS. *Environmental Science and Technology*, *33*(13), 2218–2223. https://doi.org/10.1021/es9812103

Spiliotopoulou, A., Hansen, K. M. S., & Andersen, H. R. (2015). Secondary formation of disinfection by-products by UV treatment of swimming pool water. *Science of the Total Environment*, *520*, 96–105. https://doi.org/10.1016/j.scitotenv.2015.03.044

Symons, J. M., Krasner, S. W., Simms, L. A., & Sclimenti, M. (1993). Measurement of THM and precursor concentrations revisited: the effect of bromide ion. *Journal / American Water Works Association*, *85*(1), 51–62.

Thomson, J., Roddick, F., & Drikas, M. (2002). Natural organic matter removal by enhanced photo-oxidation using low pressure mercury vapor lamps. *Water Sci. Technol.: Water Supply*, *2*(5–6), 435–443. Retrieved from http://ws.iwaponline.com.ezproxy.lib.purdue.edu/content/ppiwawstws/2/5-6/435.full.pdf

Trussell, R. R., & Umphres, M. D. (1978). The Formation of Trihalomethanes, *70*(11), 604–612.

US EPA. (n.d.). NPDWR. Retrieved from https://www.epa.gov/ground-water-and-drinking-water/national-primary-drinking-water-regulations#one

Villanueva, C. M., Cantor, K. P., Grimalt, J. O., Castaño-Vinyals, G., Malats, N., Silverman, D., … Kogevinas, M. (2006). Assessment of lifetime exposure to trihalomethanes through different routes. *Occupational and Environmental Medicine*, *63*(4), 273–277. https://doi.org/10.1136/oem.2005.023069

Villanueva, C. M., Cantor, K. P., Grimalt, J. O., Malats, N., Silverman, D., Tardon, A., … Kogevinas, M. (2006). Bladder Cancer and Exposure to Water Disinfection By-Products through Ingestion, Bathing, Showering, and Swimming in Pools. *American Journal of Epidemiology*, *165*(2), 148–156. https://doi.org/10.1093/aje/kwj364

Wang, D., Bolton, J. R., Andrews, S. A., & Hofmann, R. (2015). Formation of disinfection by-products in the ultraviolet/chlorine advanced oxidation process. *Science of The Total Environment*, *518–519*, 49–57. https://doi.org/10.1016/J.SCITOTENV.2015.02.094

Wang, H., Liu, D., Zhao, Z., Cui, F., Zhu, Q., & Liu, T. (2010). Factors influencing the formation of chlorination brominated trihalomethanes in drinking water. *Journal of Zhejiang University SCIENCE A*, *11*(2), 143–150. https://doi.org/10.1631/jzus.A0900343

Wang, W.-L., Zhang, X., Wu, Q.-Y., Du, Y., & Hu, H.-Y. (2017). Degradation of natural organic matter by UV/chlorine oxidation: Molecular decomposition, formation of oxidation byproducts and cytotoxicity. *Water Research*, *124*, 251–258. https://doi.org/10.1016/J.WATRES.2017.07.029

Watson, K., Shaw, G., Leusch, F. D. L., & Knight, N. L. (2012). Chlorine disinfection by-products in wastewater effluent: Bioassay-based assessment of toxicological impact. *Water Research*, *46*(18), 6069–6083. https://doi.org/10.1016/j.watres.2012.08.026

Weaver, W. A. (2008). Volatile disinfection by-product analysis from chlorinated indoor swimming pools. *Theses and Dissertations Available from ProQuest*. Retrieved from https://docs.lib.purdue.edu/dissertations/AAI1469786

WHO. (2004). Monochloramine in Drinking-water Background document for development of WHO Guidelines for Drinking-water Quality. Retrieved from http://www.who.int/water_sanitation_health/water-quality/guidelines/chemicals/chloramine-background.pdf

WHO. (2009). Bromide in drinking-water Background document for development of WHO Guidelines for Drinking-water Quality. Retrieved from http://www.who.int/water_sanitation_health/dwq/chemicals/Fourth_Edition_Bromide_Final_January_2010.pdf

Xu, X., Fillos, J., Ramalingam, K., & Rosenthal, A. (2012). Quantitative analysis of methanol in wastewater by GC-MS with direct injection or headspace SPME sample introduction. *Analytical Methods*, *4*(11), 3688. https://doi.org/10.1039/c2ay25452b

Zhang, C.-Y., Lin, N.-B., Chai, X.-S., Zhong-Li, & Barnes, D. G. (2015). A rapid method for simultaneously determining ethanol and methanol content in wines by full evaporation headspace gas chromatography. *Food Chemistry*, *183*, 169–172. https://doi.org/10.1016/J.FOODCHEM.2015.03.048

Zhang, J.-Y., Boyd, I. W., & Esrom, H. (1997). UV intensity measurement for a novel 222 nm excimer lamp using chemical actinometer. *Applied Surface Science*, *109–110*, 482–486. https://doi.org/10.1016/S0169-4332(96)00789-1

Zoschke, K., Börnick, H., & Worch, E. (2014). Vacuum-UV radiation at 185nm in water treatment - A review. *Water Research*, *52*, 131–145. https://doi.org/10.1016/j.watres.2013.12.034

APPENDIX

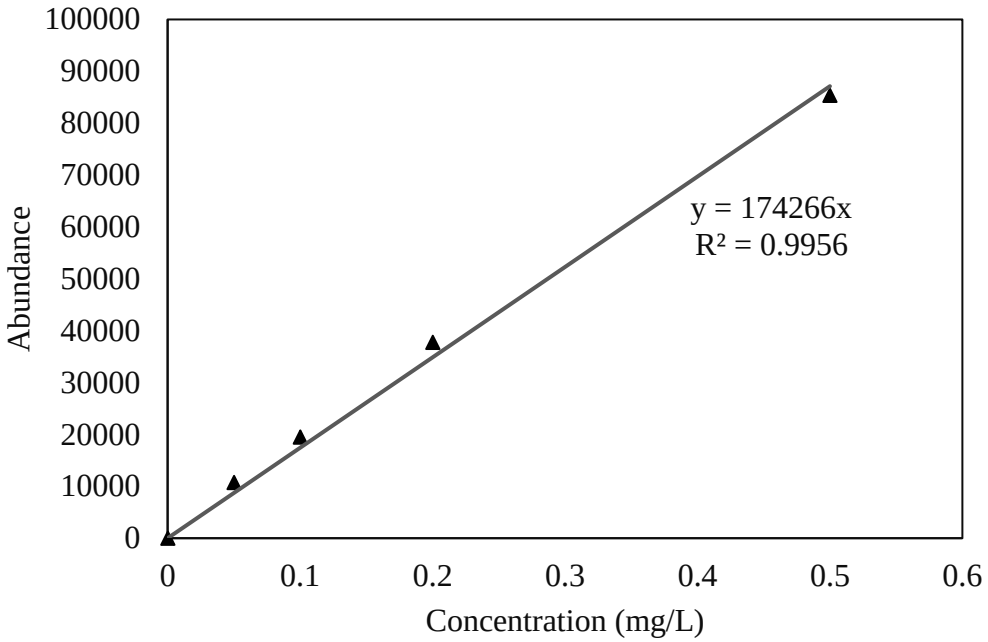

A 1 $CHCl_3$ Calibration Curve. (m/z = 83)

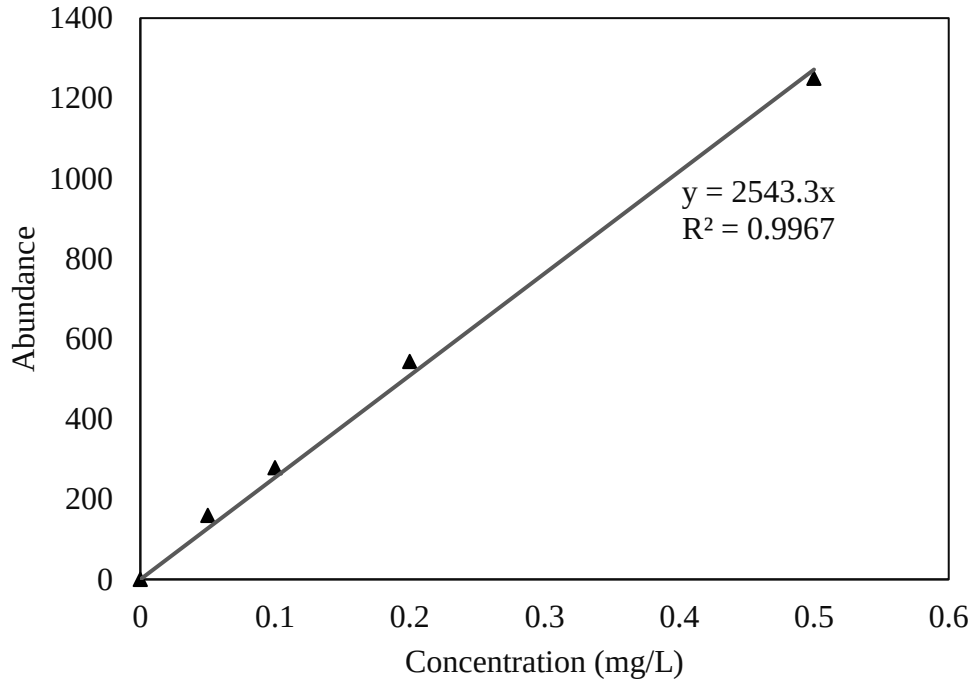

A 2 $CHCl_3$ Calibration Curve (m/z=118)

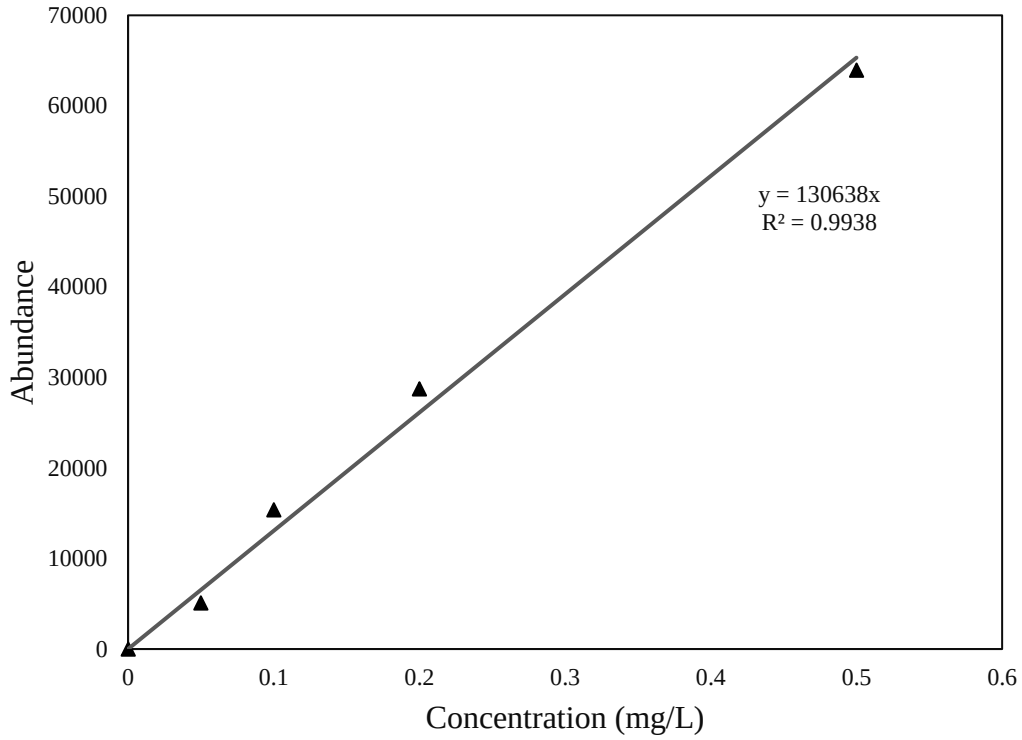

A 3 $CHBrCl_2$ Calibration Curve (m/z=83)

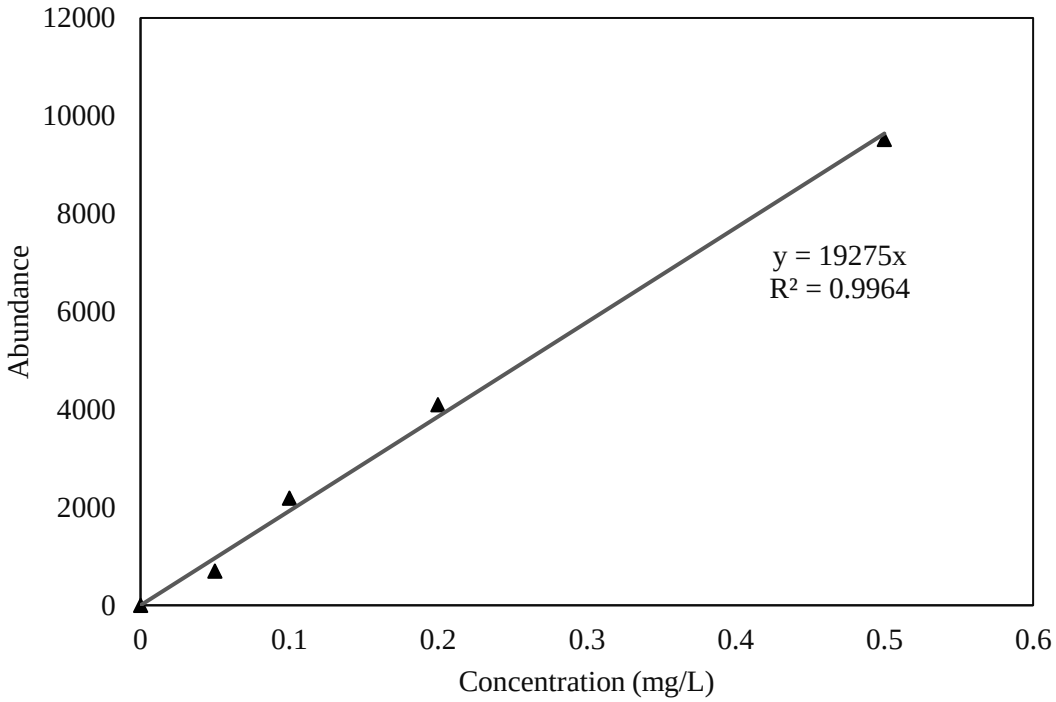

A 4 $CHBrCl_2$ Calibration Curve (m/z=129)

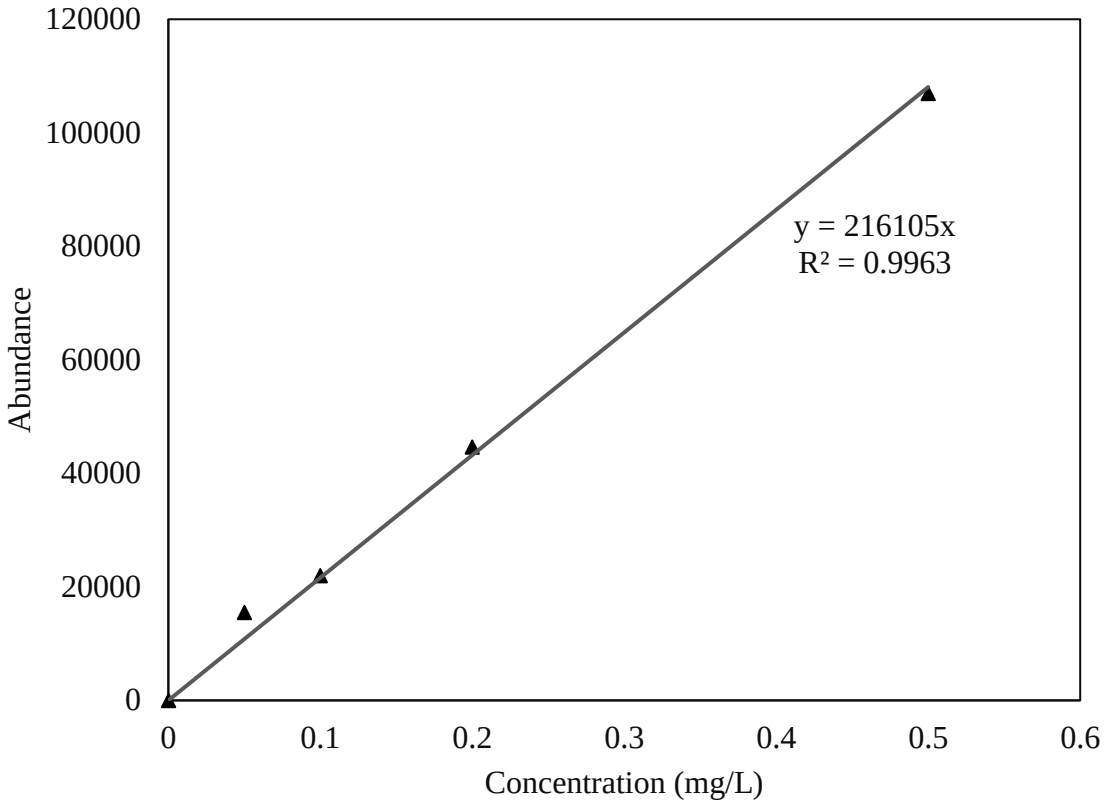

A 5 $CHClBr_2$ Calibration Curve (m/z=129)

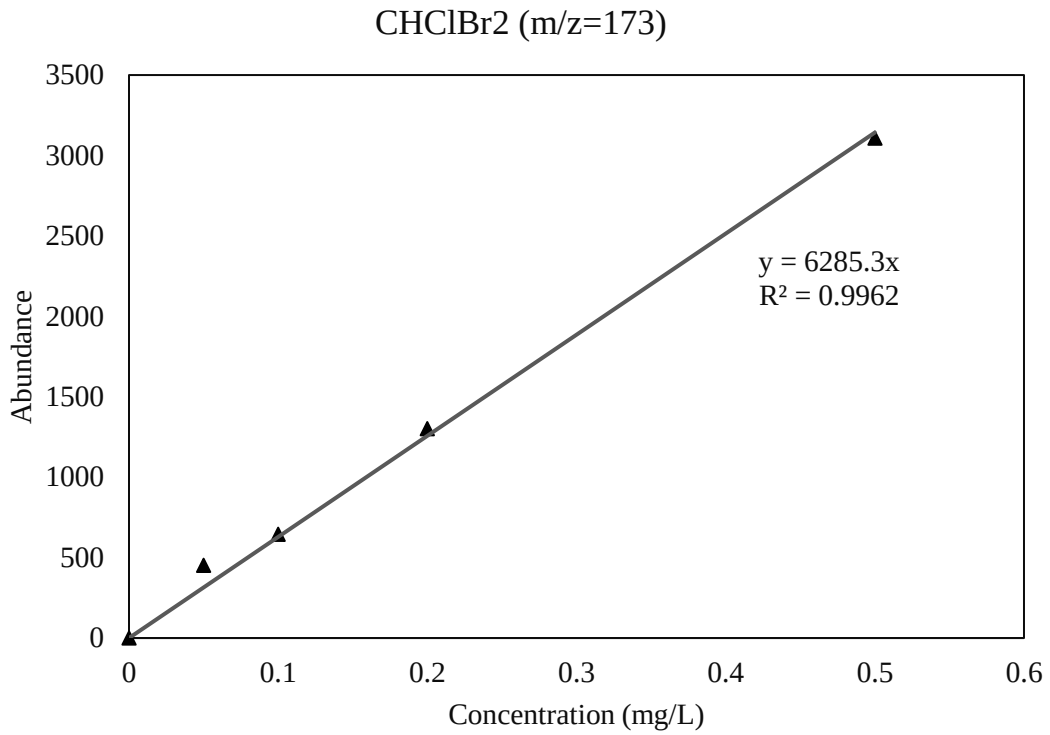

A 6 $CHClBr_2$ Calibration Curve (m/z=173)

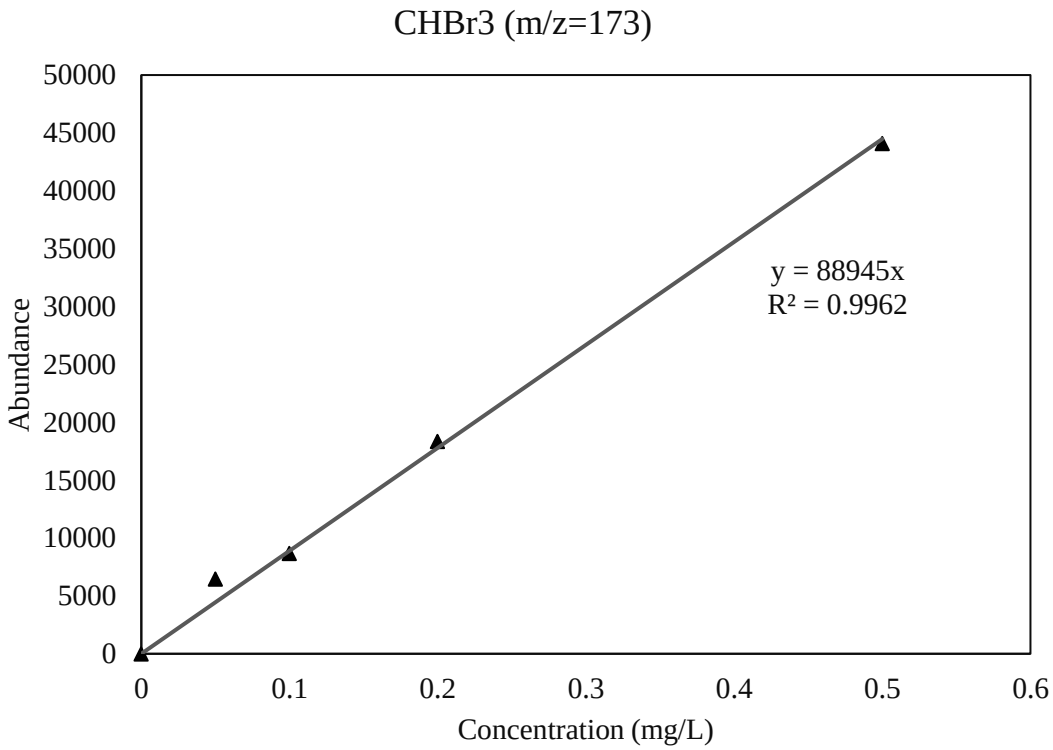

A 7 $CHBr_3$ Calibration Curve (m/z=173)

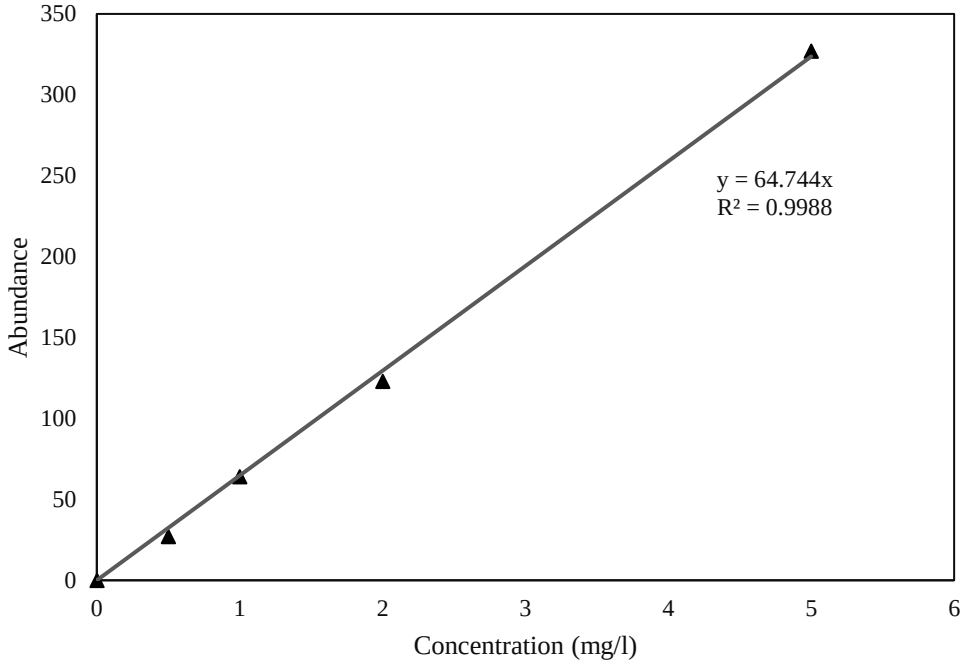

A 8 NH_2Cl Calibration Curve (m/z =53)

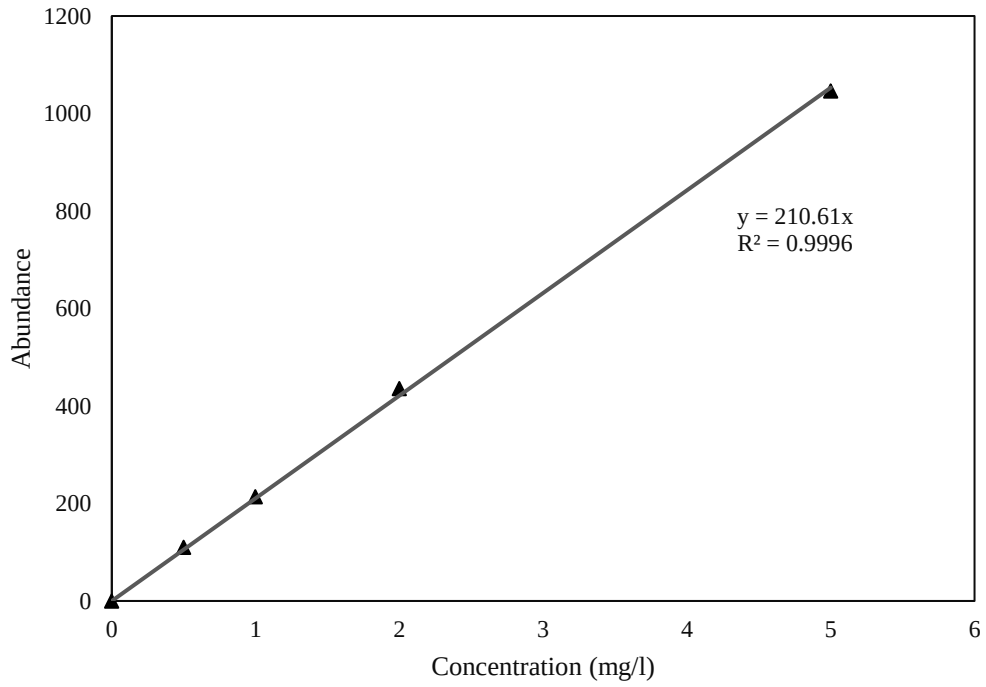

A 9 NCl_3 Calibration Curve (m/z=88)